Supporting Information for

"Bidirectional Electron Transfer Capability in Phthalocyanine–$Sc_3N@I_h$-C_{80} Complexes"

Olga Trukhina,[†,‡] Marc Rudolf,[≠] Giovanni Bottari,[†,‡] Takeshi Akasaka,*[,††] Luis Echegoyen,*[,‡‡] Tomas Torres*[,†,‡] and Dirk M. Guldi*[,≠]

[†] Department of Organic Chemistry, Universidad Autónoma de Madrid, Cantoblanco, 28049 Madrid (Spain)

[‡] IMDEA Nanociencia, Faraday 9, 28049 Madrid (Spain)

[≠] Department of Chemistry and Pharmacy and Interdisciplinary Center for Molecular Materials (ICMM), Friedrich-Alexander-Universität Erlangen-Nürnberg, 91058 Erlangen (Germany)

[††] Department of Chemistry, Tokyo Gakugei University, Koganei, Tokyo 184-8501 (Japan)

[‡‡] Department of Chemistry, University of Texas at El Paso, El Paso, TX 79968 (USA)

Table of Content

1. General and methods

Chemicals (reagent grade) as well as solvents (anhydrous, deuterated and HPLC grade) were purchased from Aldrich Chemical, Alfa Aesar and Scharlau and used as received without further purification. Glassware was oven-dried at 110 ^{o}C overnight before use. Column chromatography was carried out using silica gel Merck-60 (230-400 mesh, 60 Å) as the solid support. Thin layer chromatography (TLC) analyses were performed on aluminum sheets precoated with silica gel 60 F254 (Merck). High-performance liquid chromatography (HPLC) was performed on an Agilent 1100 LC (Agilent Technologies), using ø 4.6 × 250 mm Buckyprep column (Cosmosil). A mixture of toluene/*o*-dichlorobenzene (*o*-DCB)/methanol/NEt_3 = 75:25:1:1, vol %, at 0.7 mL/min flow rate and detection wavelength of 390 nm was employed. Matrix-assisted laser desorption ionization time-of-flight (MALDI-TOF) experiments were carried out using Bruker Ultraflex III mass spectrometer, in both positive and negative ion modes. A convenient matrix for these measurements is indicated for each compound. NMR spectra were measured on a Bruker ASCEND-400 or a Bruker AVANCE 3HD NMR-700 spectrometer, locked on deuterated solvents. Carbon chemical shifts are measured in ppm relative to trimethylsilane (TMS), using the resonance of the deuterated solvent as an internal standard. The assignment of the NMR signals was supported, in some cases, by 2D-NMR spectra such as HSQC, HMBC (700 MHz). UV-Vis spectra were recorded on a Varian Cary 50 Conc spectrophotometer using spectroscopic grade solvents in 1 cm path length quartz cell.

Steady-State Emission. The spectra were recorded on a FluoroMax 3 fluorometer (HORIBA JobinYvon). The measurements were carried out at room temperature.

Time-Resolved Absorption. Femtosecond transient absorption studies were performed with 387 and 676 nm laser pulses (1 kHz, 150 fs pulse width) from an amplified Ti:Sapphire laser system (CPA-2101 from Clark-MXR, Inc.), the laser energy was 200 nJ.

Electrochemistry. Cyclic voltammetry (CV) and square wave voltammetry (SWV) studies were performed on an Autolab PGSTAT30 potentiostate/galvanostate. Measurements were carried out in a home-built one-compartment cell using a three-electrode configuration, *o*-DCB as a solvent and 0.05 M tetra-*n*-butylammonium hexafluorophosphate (*n*-Bu_4NPF_6) as supporting electrolyte. A platinum electrode was used as the working electrode, a platinum wire as a counter electrode, $Ag/AgNO_3$ non-aqueous electrode as a reference. All potentials were recorded against a $Ag/AgNO_3$ non-aqueous electrode and corrected against Fc^+/Fc redox couple. CV was measured at scan rates of 100 mVs^{-1} and 50 mVs^{-1}, SWV was measured at scan rates of 50 mVs^{-1} and 20 mVs^{-1}. Prior to each voltammetric measurement, the cell was degassed by bubbling with argon for about 20 min. Electrochemical measurements were performed at a concentration of

approximately 1×10^{-3} M for compounds **1**−**3**, and 1×10^{-5} M for compound **4**[*]. Compensation for internal resistance was not applied.

2. Synthesis and characterization of derivatives 1-4

N-(*p*-pyridyl)-3,4-C_{60} fulleropyrrolidine derivative **3**,[1] and Sc_3N@*Ih*-C_{80} fullerene (>99%)[2] were prepared according to the synthetic procedure reported elsewhere; tetra-*tert*-butyl Zn(II)Pc **1** was purchased from Sigma Aldrich.

[5,6]-*N*-(*p*-pyridyl)-3,4-Sc_3N@*Ih*-C_{80} fulleropyrrolidine, alias derivative **4**:

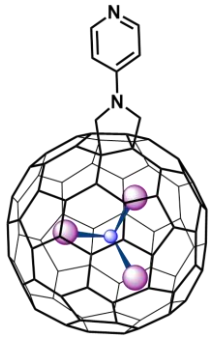

Argon was bubbled through a mixture of 3.0 mg of Sc_3N@*Ih*-C_{80} (2.7 μmol, 1 eq) and 15.0 mg of *N*-pyridylglycine (98 μmol, 35 eq) in 12 mL of *o*-DCB upon sonication for 15 min. After this time, the mixture was heated to reflux under argon for 10 minutes and a slurry of 15 mg of paraformaldehyde (0.5 mmol, 185 eq) in 4 mL of *o*-DCB added in three portions every 15 min. Once the addition was complete the reaction mixture was heated to reflux for the next 12 h, following the reaction by HPLC (aliquots were taken every 15 minutes in order to estimate the ratio between the [5,6] and the [6,6] monoaddutcs). The reaction was stopped when the presence of the [6,6]-adduct was not observed anymore by HPLC. The resulting reaction mixture was then allowed to cool down to room temperature and charged onto silica gel column, eluting first with *o*-DCB in order to remove the unreacted Sc_3N@*Ih*-C_{80} fullerene, followed by a 10:1 mixture of *o*-DCB/NEt_3 in order to elute [5,6]-adduct **4**.[†] The column chromatography fractions containing **4** were then reduced in volume under vacuum until reaching a volume of 10 mL. This latter solution was then washed with 15 mL of saturated solution of sodium bicarbonate (x 1 time) and 15 mL of distilled water (x 3 times). The resulting organic layer was dried over Na_2SO_4 and filtered. The filtrate was then reduced in volume until dryness and the obtained solid washed with diethyl ether and hexane, and the product finally dried under vacuum. Yield: 0.4 mg (12%; 20% on the basis of the recovered Sc_3N@*Ih*-C_{80} fullerene). HPLC retention time = 120 min; ^{1}H-NMR (CS_2:CD_2Cl_2 2:1, 400 MHz): δ (ppm) = 8.44 (m, 2H), 6.91 (m, 2H), 4.89 (d, *J* = 10.8 Hz, 2H), 3.82 (d, *J* = 10.8 Hz, 2H); MALDI-TOF

[*] In the case of Sc_3N@*Ih*-C_{80} derivative **4**, a lower concentration was used for the electrochemical studies due to the reduced solubility of this fullerene derivative in *o*-DCB.

[†] A negligible formation of Sc_3N@*Ih*-C_{80} bisadducts could be detected by TLC on silica plates eluting with *o*-DCB/NEt_3 (10:1) once the reaction was stopped. These bisadducts were not detected by HPLC, probably, due to their long retention times. During the column chromatography, after the eluting mixture was changed to *o*-DCB/DMF 1:1, a negligible amount of a very polar fullerene-based compound was collected. The MALDI-TOF mass spectrometry spectrum of this column chromatography fraction confirmed, beside the presence of monoadduct **4**, the presence of Sc_3N@*Ih*-C_{80} bisadducts and minor amounts of product degradation, a degradation probably occurring during the mass spectrometry experiment (Figure S4).

MS (negative ionization, 9-nitroanthracene): found: 1228.9 *m/z*, calc. for $C_{87}H_8N_3Sc_3$, $[M]^-$: 1228.9, found: 1108.9 *m/z*, calc. for $C_{80}NSc_3$, $[M]^-$: 1108.9, found: 1165.9 *m/z*, calc. for $C_{83}H_7N_2Sc_3$, $[M]^-$: 1165.9; UV-vis (*o*-DCB): λ_{max} (nm) (log ε) = 316 (4.2), 372 (sh), 420 (sh), 471 (sh).

[6,6]-*N*-(*p*-pyridyl)-3,4-Sc_3N@*Ih*-C_{80} fulleropyrrolidine:

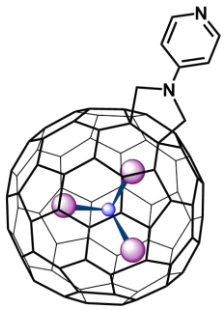

The [6,6]-adduct of *N*-(*p*-pyridyl)-3,4-Sc_3N@*Ih*-C_{80} fulleropyrrolidine, being the kinetically controlled product, was detected by HPLC as the major product 15 min after the reaction started, together with minor amounts of the [5,6]-adduct **4** (*i.e.*, [5,6]/[5,6] ratio 87/13). The isolation of the [6,6]-adduct was not performed due to its full conversion into the [5,6]-isomer **4** along the reaction course (12 h at reflux). However, the ^{1}H-NMR spectral features of the [6,6]-adduct were obtained from a 25/75 mixture of the [6,6]-/[5,6]-isomers sampled 6h after the beginning of the reaction. HPLC retention time = 160 min.; ^{1}H-NMR (700 MHz, CS_2/CD_2Cl_2 (2:1), capillary): δ (ppm) = 8.34-8.32 (m, 2H), 6.74-6.72 (m, 2H), 4.28 (s, 2H), 3.97 (s, 2H).

2,3,9,10,16,17,23,24-octakis-pentylsulfonyl Zn(II)Pc **2**:

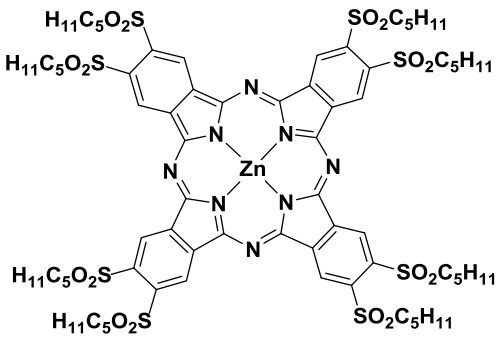

A mixture of 50 mg of 1,2-dicyano-4,5-bis(pentylsulfonyl)benzene (0.126 mmol, 2.7 eq) and 8.5 mg of $Zn(OAc)_2$ (0.046 mmol, 1 eq) was heated to 145 ºC in 1.2 mL of a *o*-DCB/DMF (5:1) mixture under argon atmosphere. The reaction completed in 26 h being followed by TLC. After being cooled to room temperature, the reaction mixture was evaporated to dryness under vacuum and the residue was triturated in hexane. The suspension was then filtered and the solid dissolved in 3 mL of $CHCl_3$. This chloroform solution was then charged onto silica gel column eluted with a mixture of $CHCl_3$/ethyl acetate (100:1) which allowed to obtain Zn(II)Pc **2** as a green solid compound after solvent removal. Finally, electron-donating Zn(II)Pc **2** was recrystallized from DCM with a small addition of hexane, filtered, washed with cold hexane and dried under vacuum. Yield: 28 mg (54%). ^{1}H-NMR (400 MHz, THF-d_8): δ (ppm) = 10.36 (s, 8H; H-1, H-4, H-8, H-11, H-15, H-18, H-22, H-25), 4.25-3.91 (m, 16H; SO_2CH_2), 2.23-1.95 (m, 16H; $SO_2CH_2C\underline{H}_2$), 1.66-1.36 (m, 32H; $SO_2(CH_2)_2(C\underline{H}_2)_2$), 0.97-0.94 (m, 24H; CH_3); ^{13}C-NMR (THF-d_8, 100.6 MHz): δ (ppm) = 154.52 (8C; C-5, C-7, C-12, C-14, C-19, C-21, C-26, C-28), 142.37 (8C; C-2, C-3, C-9, C-10, C-16, C-17, C-23, C-24), 141.73 (8C; C-4a, C-7a,

C-11a, C-14a, C-18a, C-21a, C-25a, C-28a), 128.95 (8C; C-1, C-4, C-8, C-11, C-15, C-18, C-22, C-25), 57.68 (8C; SO_2CH_2), 31.39 (8C; $SO_2CH_2\underline{C}H_2$), 23.00 (8C; $SO_2(CH_2)_2\underline{C}H_2$), 22.64 (8C; $SO_2(CH_2)_3\underline{C}H_2$), 14.04 (8C; CH_3); MALDI-TOF MS (positive mode, DCTB): found: 1648.3 *m/z*, calc. for $C_{72}H_{96}N_8O_{16}S_8Zn$, $[M]^+$: 1648.4, found: 1671.3 *m/z*, calc. for $C_{72}H_{96}N_8NaO_{16}S_8Zn$, $[M+Na]^+$: 1671.4, found: 3296.9 *m/z*, calc. for $C_{144}H_{192}N_{16}O_{32}S_{16}Zn_2$, $[2M]^+$: 3296.8, found: 3319.9 *m/z*, calc. for $C_{144}H_{192}N_{16}NaO_{32}S_{16}Zn_2$, $[2M+Na]^+$: 3319.8; UV-vis (THF): λ_{max} (nm) (log ε) = 683 (5.5), 659 (sh), 622 (4.6), 431 (sh), 378 (4.7), 341 (4.7).

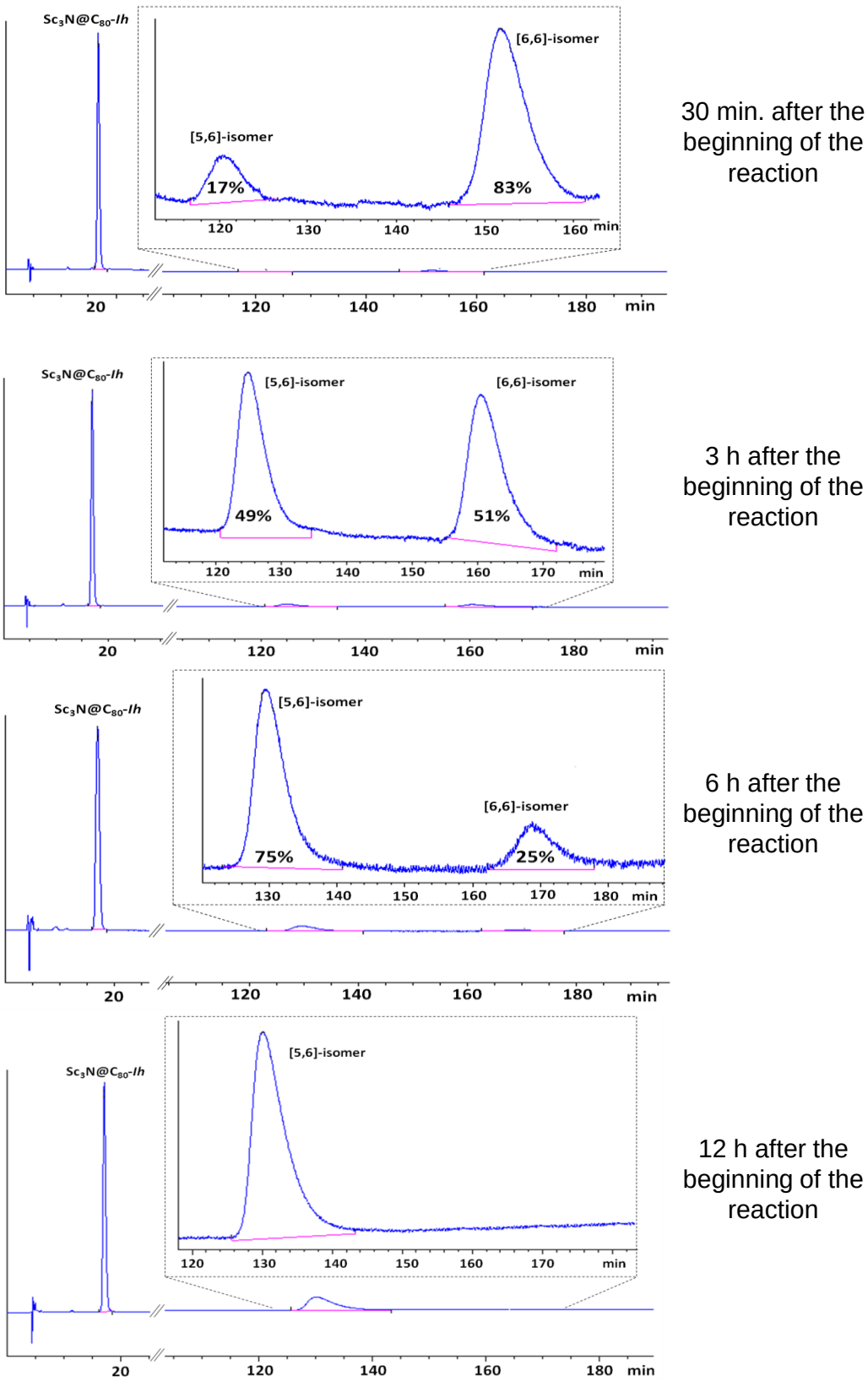

Figure S1: HPLC profiles of four aliquots taken from the reaction mixture leading to $Sc_3N@I_h$-C_{80} derivative **4** at different reaction times (*i.e.*, 30 min, 3h, 6h and 12 h, from top to bottom). Buckyprep column (ø 4.6 × 250 mm, Cosmosil, toluene/*o*-DCB/methanol/NEt_3 (75:25:1:1, vol %) at 0.7 mL/min flow rate and detection wavelength of 390 nm.

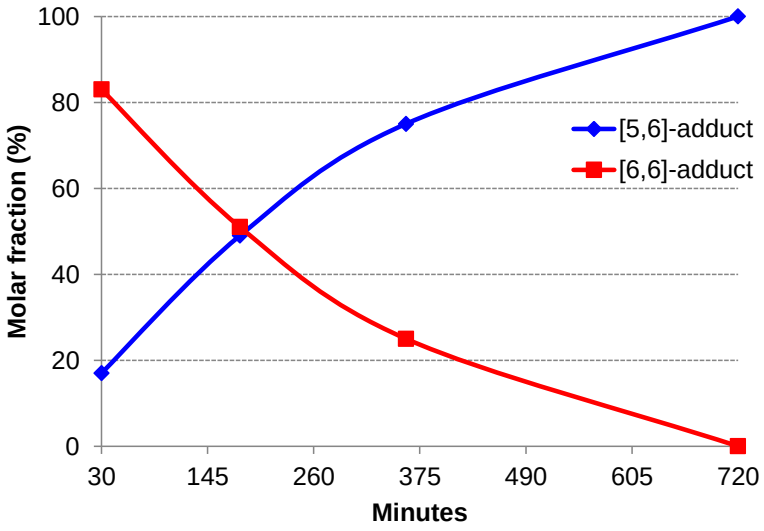

Figure S2: Molar fraction (as obtained by HPLC) of the kinetically-controlled [6,6]-adduct (blue rhombs) and the thermodynamically-controlled [5,6]-adduct (red squares) within the reaction mixture leading to $Sc_3N@I_h$-C_{80} derivative **4** as a function of the reaction time.

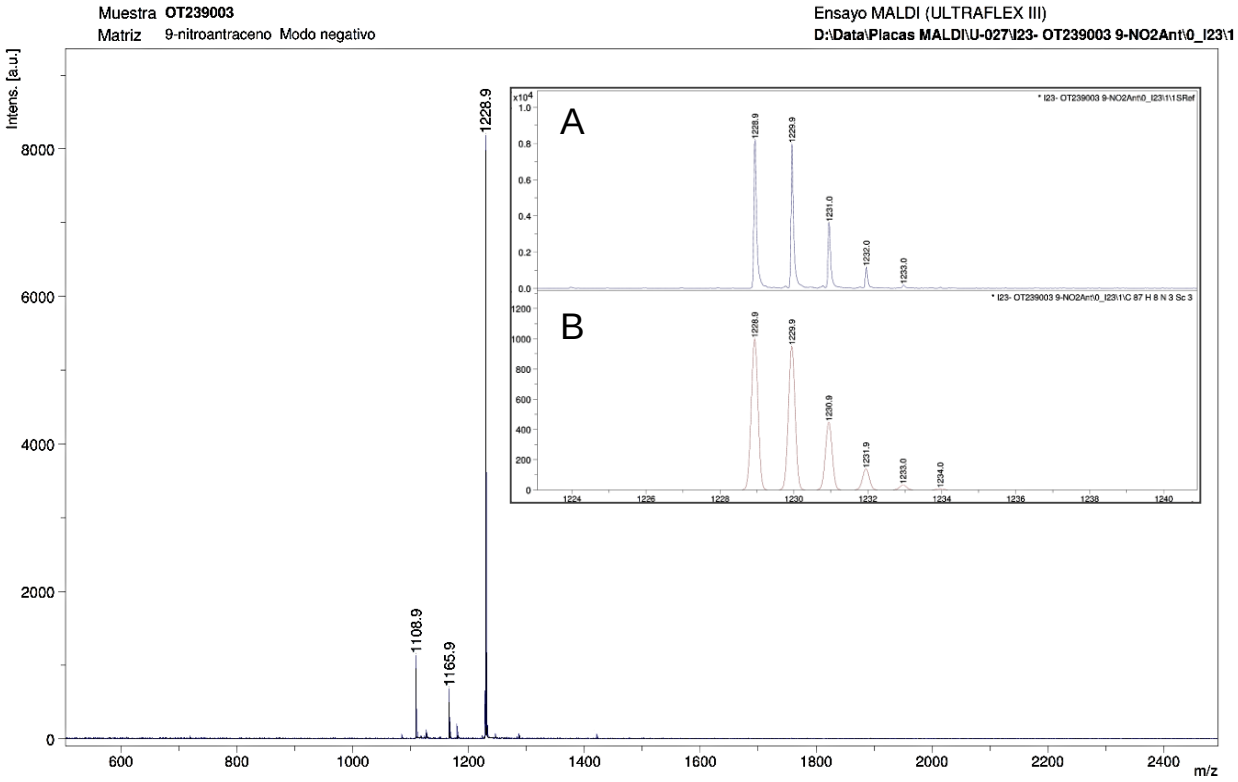

Figure S3*:* MALDI-TOF mass spectrum (9-nitroanthracene, negative mode) of $Sc_3N@Ih$-C_{80} derivative **4**. Inset: A, isotopic resolution of the MALDI-TOF peak maximizing at 1228.9 *m/z*. B, calculated isotopic pattern for compound **4** (FW = $C_{87}H_8N_3Sc_3$, MW = 1229,9).

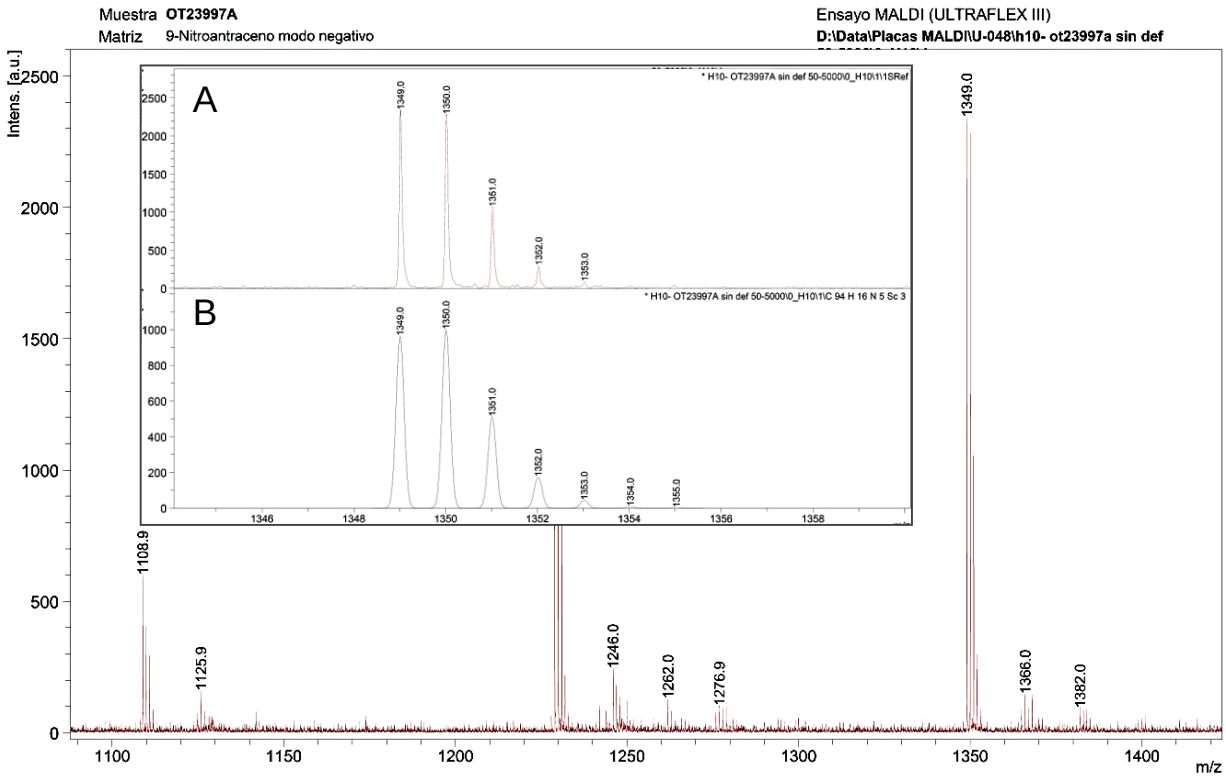

Figure S4: MALDI-TOF mass spectrum (9-nitroanthracene, negative mode) of a column chromatography fraction of the reaction leading to Sc_3N@*Ih*-C_{80} derivative **4**, confirming the formation of Sc_3N@*Ih*-C_{80} bisadducts. Inset: A, isotopic resolution of the MALDI-TOF peak maximizing at 1349.0 *m/z*. B, calculated isotopic pattern for a bis(*N*-(*p*-pyridyl))-3,4-Sc_3N@*Ih*-C_{80} fulleropyrrolidine bisadduct (FW = $C_{94}H_{16}N_5Sc_3$, MW = 1350,1).

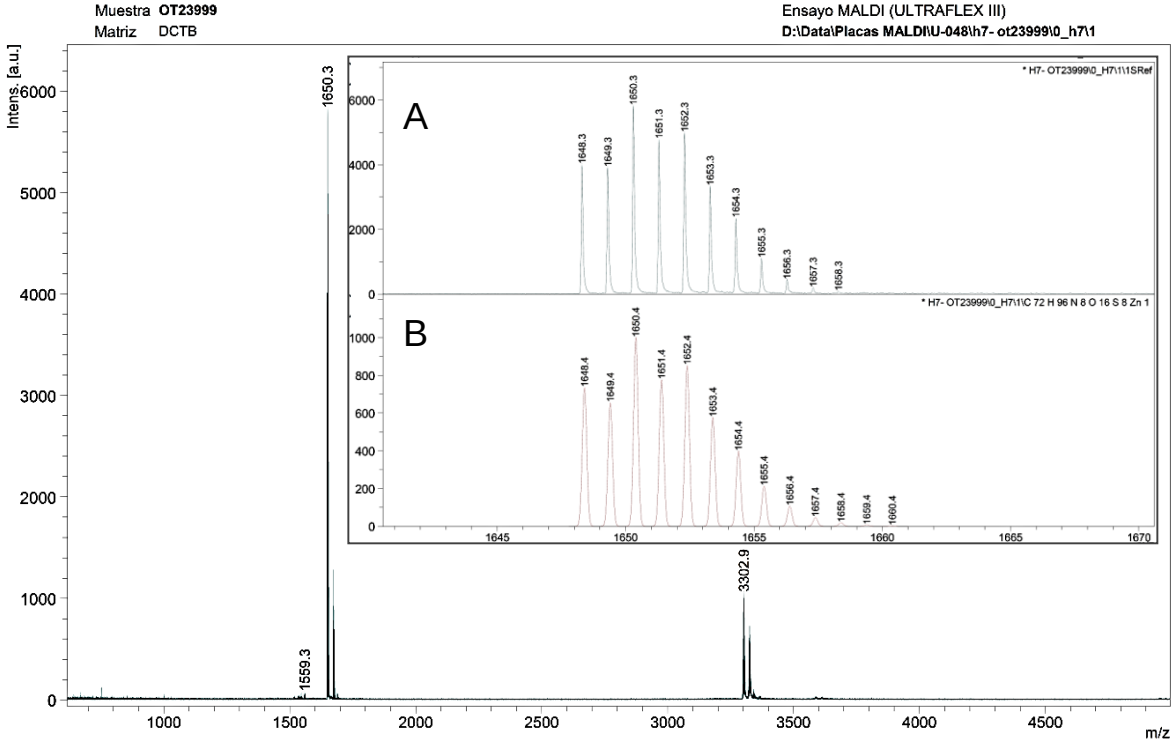

Figure S5*:* MALDI-TOF mass spectrum (DCTB, positive mode) of electron-deficient Zn(II)Pc **2**. Inset: A, isotopic resolution of the MALDI-TOF peak maximizing at 1650.3 *m/z*. B, calculated isotopic pattern for compound **2** (FW = $C_{72}H_{96}N_8O_{16}S_8Zn$, MW = 1651,5).

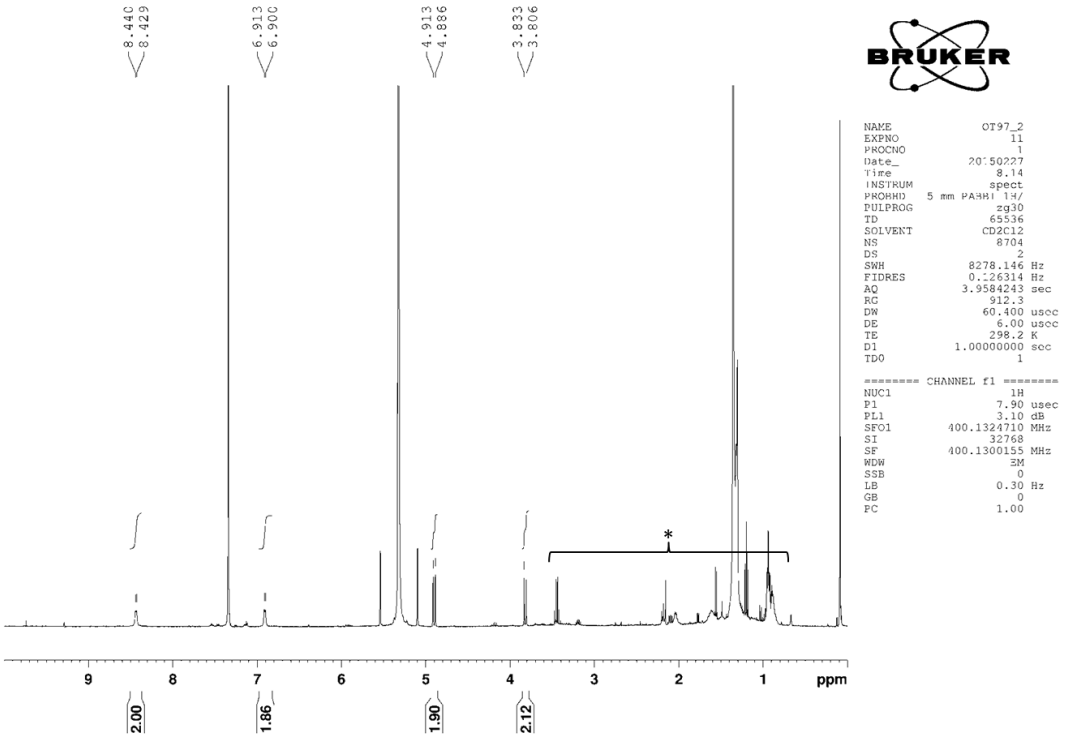

Figure S6: ^{1}H-NMR spectrum (400 MHz, CS_2/CD_2Cl_2 2:1) of $Sc_3N@I_h$-C_{80} derivative **4** (impurities in the CS_2/CD_2Cl_2 mixture are marked with an asterisk).

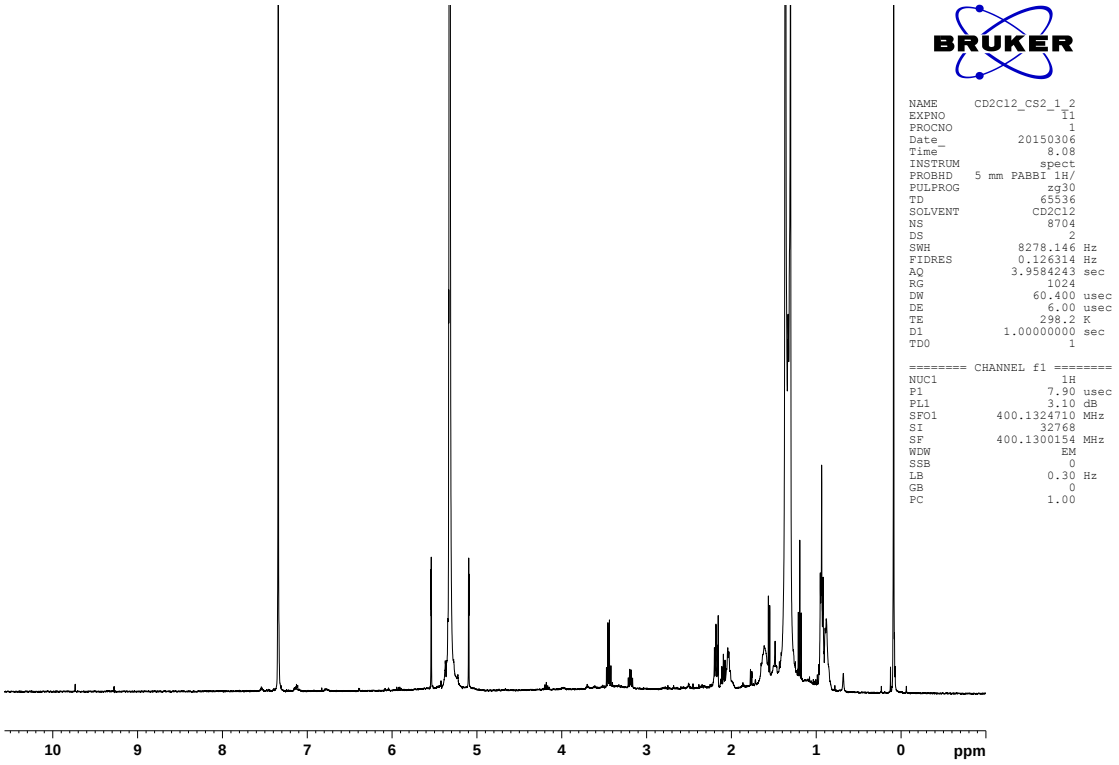

Figure S7*:* ^{1}H-NMR spectrum (400 MHz) of a 2:1 CS_2/CD_2Cl_2 mixture, revealing impurities observed in the spectrum of $Sc_3N@I_h$-C_{80} derivative **4** in the same solvents mixture (*i.e.*, Figure S6).

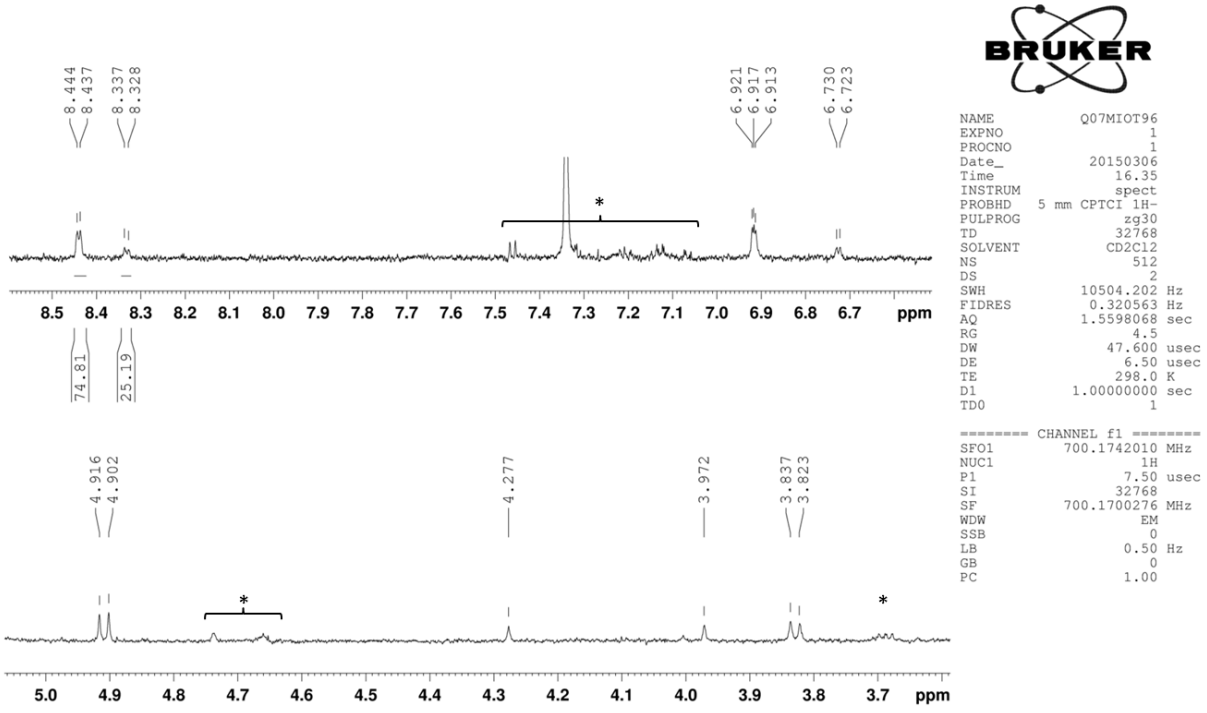

Figure S8*:* ^{1}H-NMR spectrum (700 MHz, CS_2/CD_2Cl_2 (2:1), capillary) of a 25:75 mixture of [6,6]- and [5,6]-*N*-(*p*-pyridyl)-3,4-$Sc_3N@Ih$-C_{80} fulleropyrrolidine isomers (impurities in the CS_2/CD_2Cl_2 mixture are marked with an asterisk).

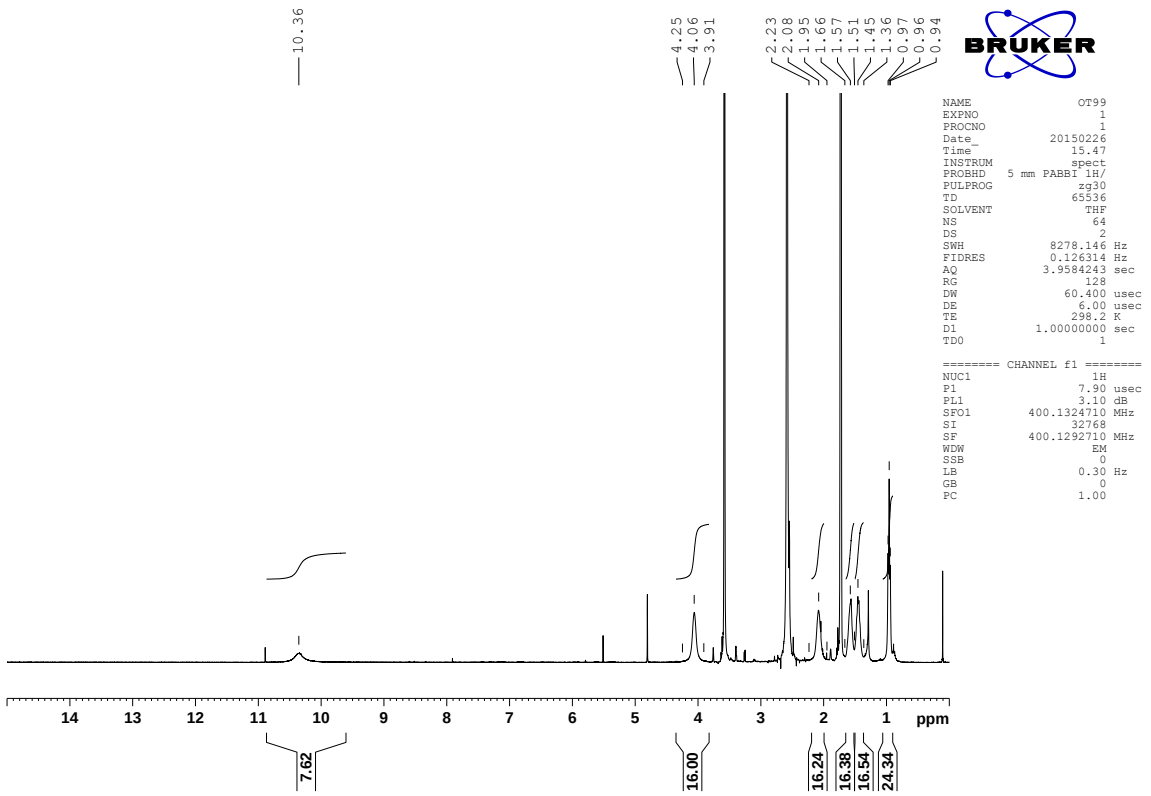

Figure S9*:* ^{1}H-NMR spectrum (400 MHz, THF-d_8) of electron-deficient Zn(II)Pc **2**.

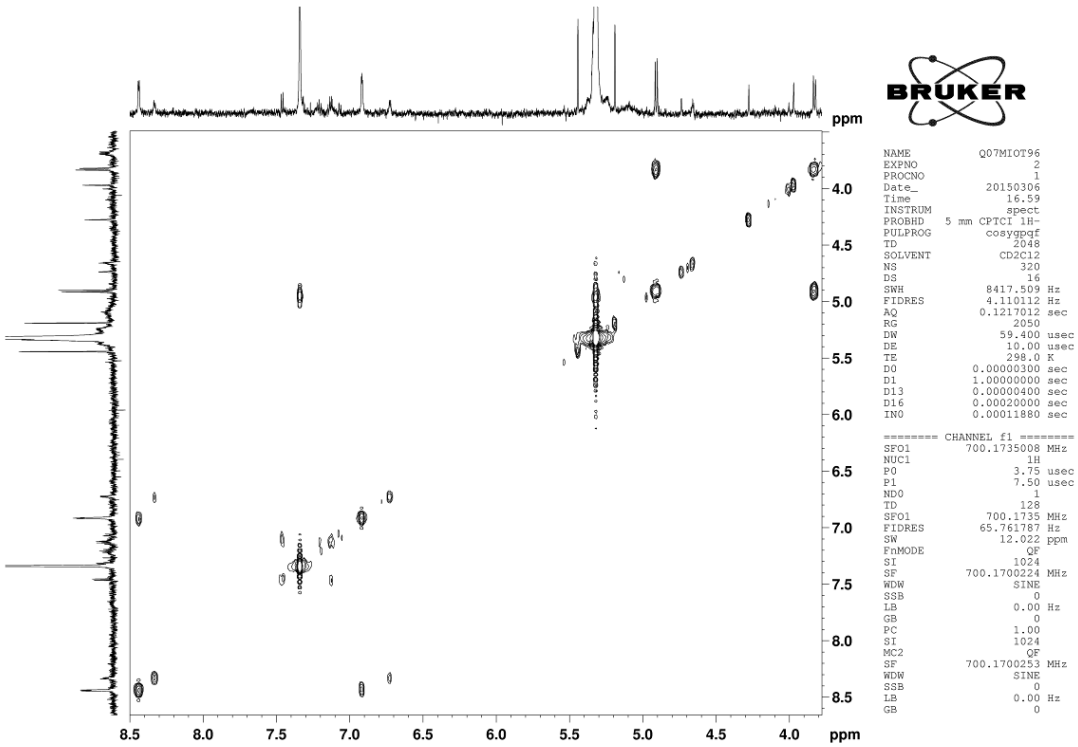

Figure S10*:* COSY-NMR spectrum (700 MHz, CS_2/CD_2Cl_2 (2:1), capillary) of a 25:75 mixture of [6,6]- and [5,6]-*N*-(*p*-pyridyl)-3,4-Sc_3N@*Ih*-C_{80} fulleropyrrolidine isomers.

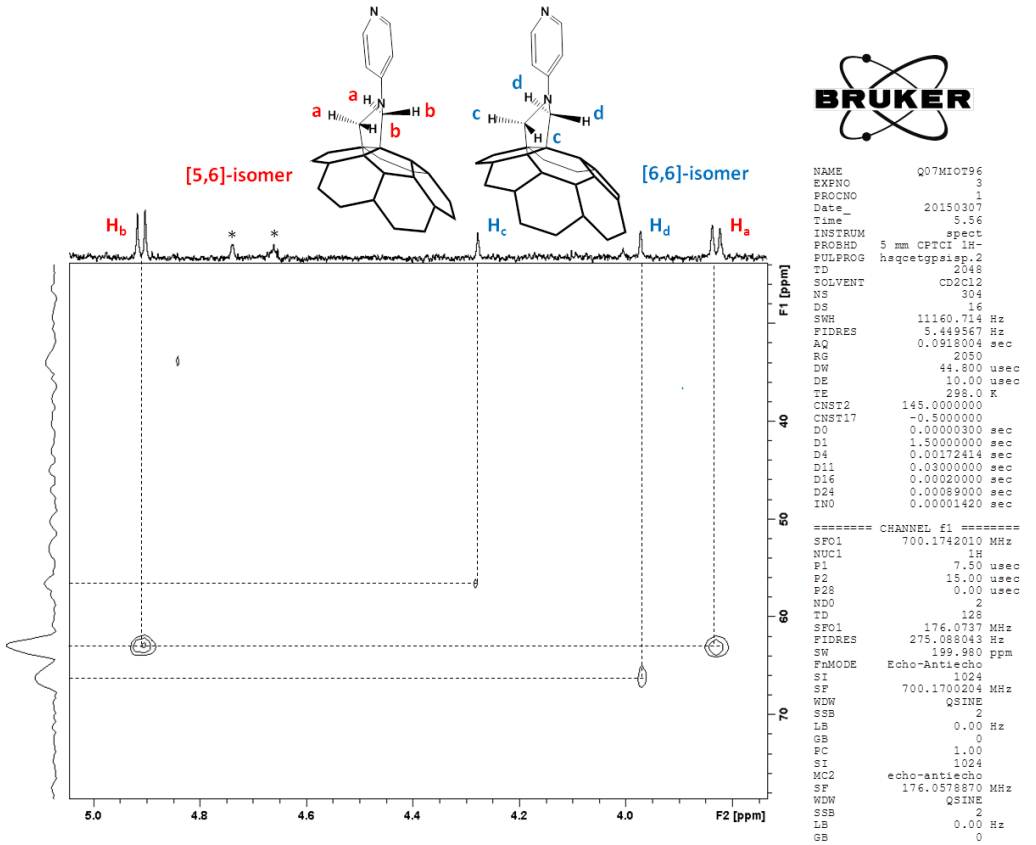

Figure S11: ^{1}H-^{13}C HSQC NMR spectrum (700 MHz, CS_2/CD_2Cl_2 (2:1), capillary) of a 25:75 mixture of [6,6]- and [5,6]-*N*-(*p*-pyridyl)-3,4-Sc_3N@*Ih*-C_{80} fulleropyrrolidine isomers.

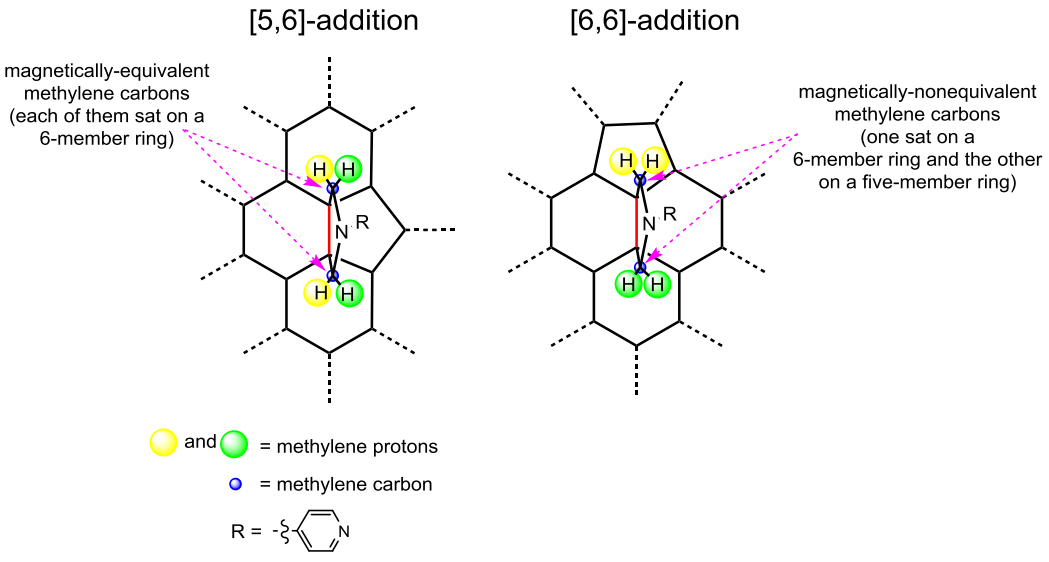

Figure S12: Schematic representation of the [5,6]- and [6,6]-addition patterns of the [5,6]- and [6,6]-*N*-(*p*-pyridyl)-3,4-Sc_3N@*Ih*-C_{80} fulleropyrrolidine isomers, respectively. Highlighted in red is the carbon-carbon bond shared i) between the Sc_3N@*Ih*-C_{80} cage and the pyrrolidine ring and ii) between a five- and a six-membered ring in the case of the [5,6]-addend, and two six-

membered rings in the case of the [6,6]-addend. Highlighted in yellow and green are the geminal pyrrolidine methylene protons which are magnetically equivalent in the case of the [5,6]-addend and magnetically nonequivalent in the case of the [6,6]-addend. On the other hand, the two methylene carbon atoms, marked in blue, are magnetically equivalent in the case of the [5,6]-addend (both carbon atoms are sat on top of a six-membered ring) and magnetically nonequivalent in the case of the [6,6]-addend (one carbon atom is sat on top of a six-membered ring and the other on top of a five-membered ring).

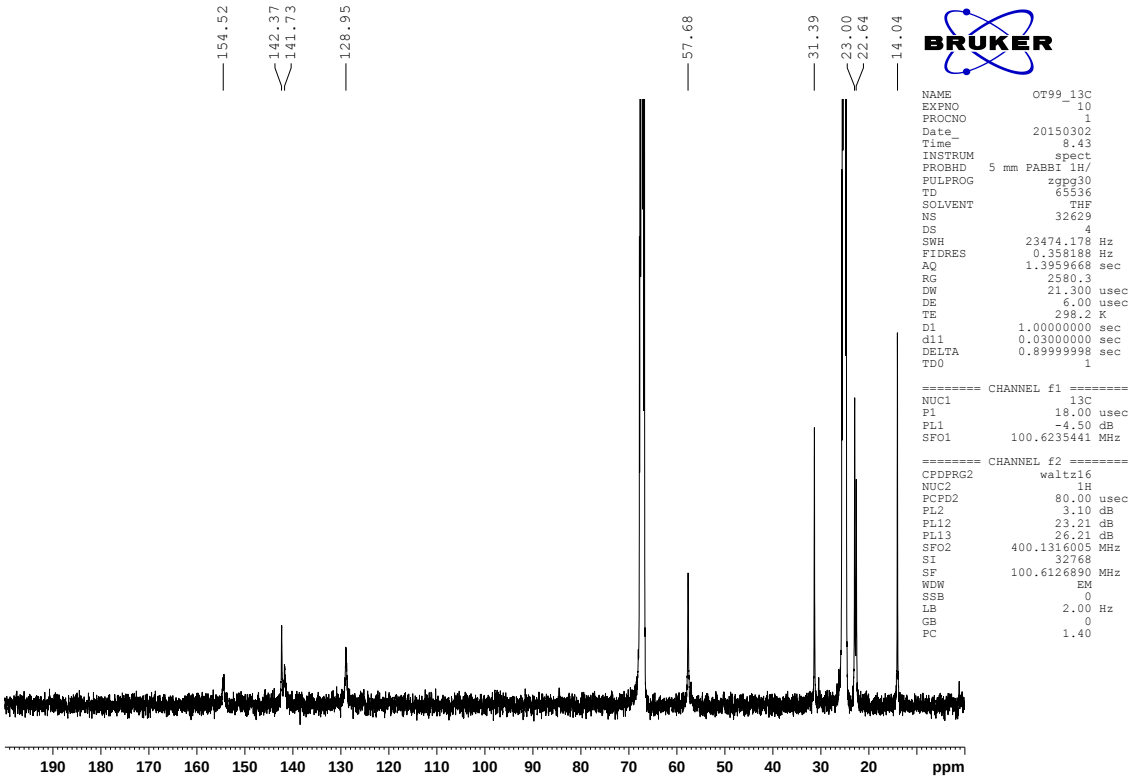

Figure S13: ^{13}C-NMR spectrum (100.6 MHz, THF-d_8) of electron-deficient Zn(II)Pc **2**.

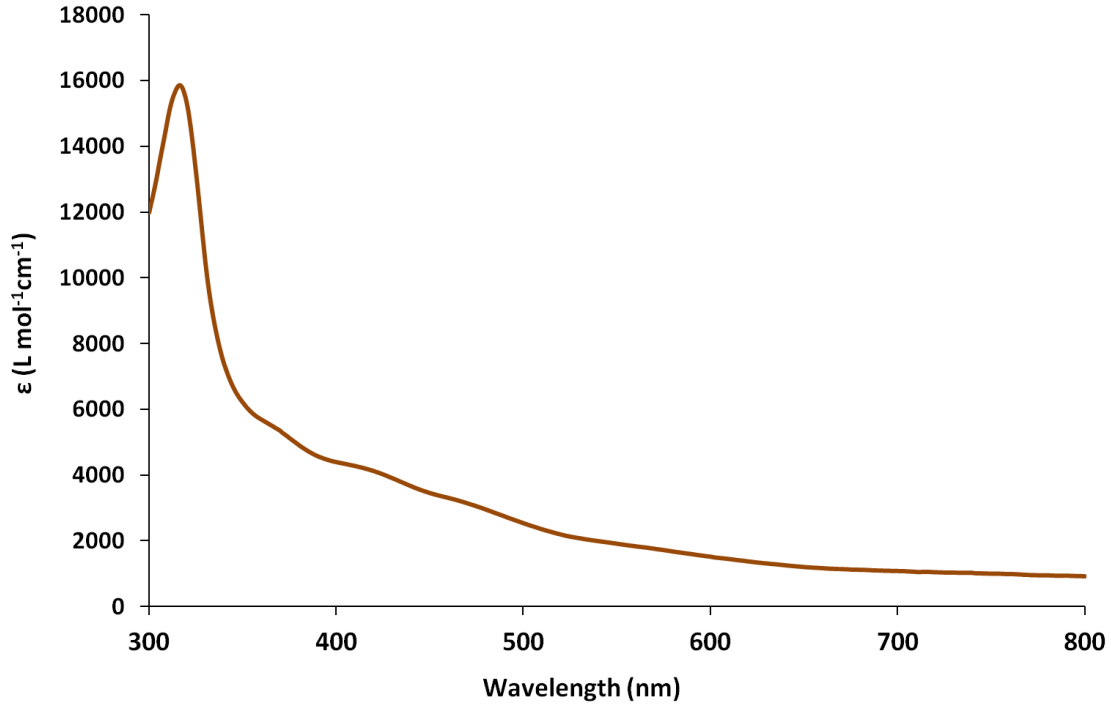

Figure S14*:* UV-vis spectrum of $Sc_3N@I_h$-C_{80} derivative **4** in *o*-DCB.

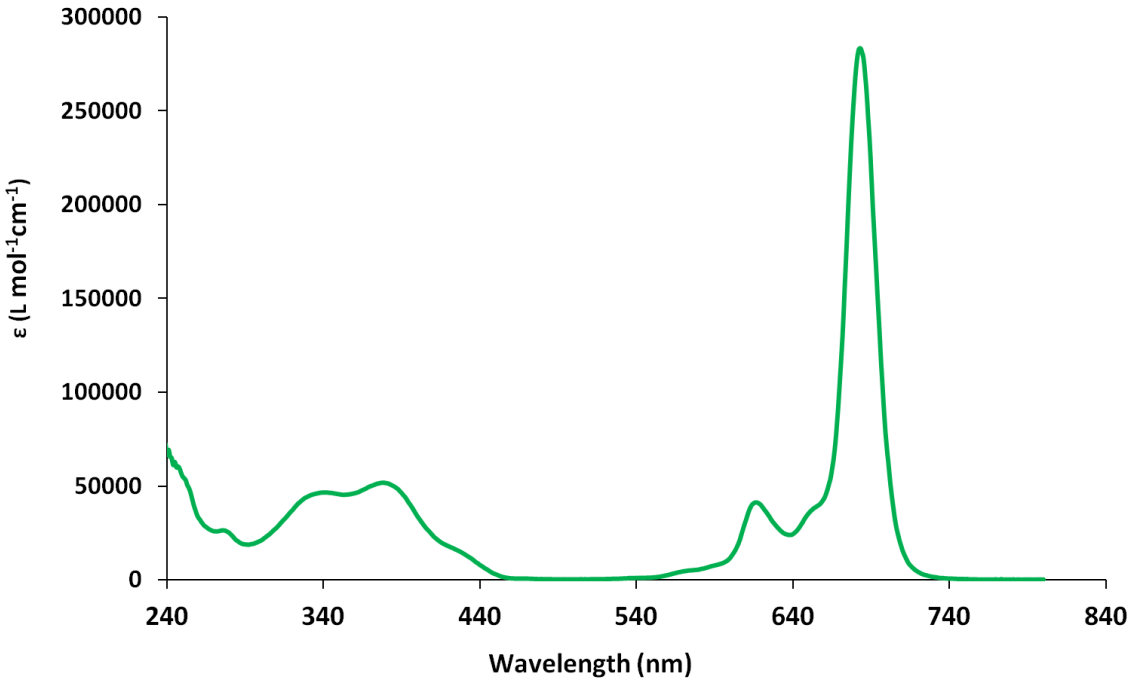

Figure S15: UV-vis spectrum of electron-deficient Zn(II)Pc **2** in THF.

3. Electrochemical studies on derivatives 1-4

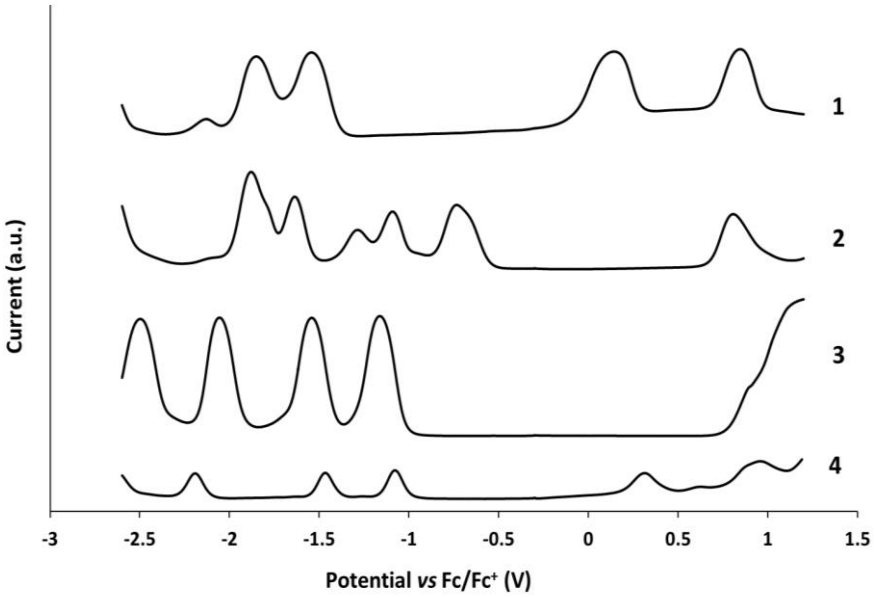

Figure S16: Square wave voltammogramms of derivatives **1**–**3** ($c \approx 10^{-3}$ M) and **4** ($c \approx 10^{-5}$ M)‡ at 20 mVs^{-1} in *o*-DCB with 0.05 M *n*-Bu_4NPF_6 as a supporting electrolyte, Pt electrode as working electrode, Pt wire as counter electrode, $Ag/AgNO_3$ non-aqueous electrode as pseudo-reference electrode. Potential values are referred to $E_{(ox)1/2}$ of the Fc/Fc^+ redox couple (+0.30 V in the present conditions).

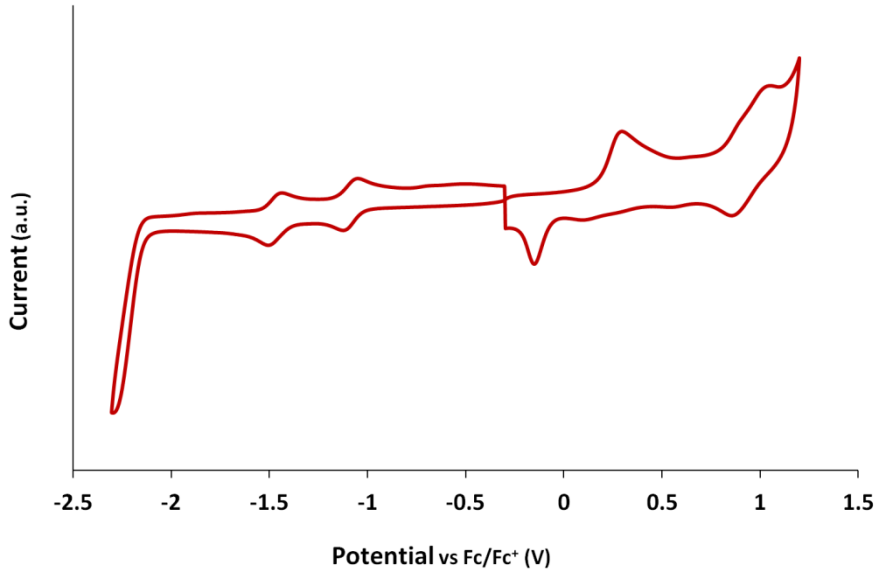

Figure S17: Cyclic voltammogram of $Sc_3N@I_h$-C_{80} derivative **4** ($c \approx 10^{-5}$ M) at 50 mVs^{-1} in *o*-DCB with 0.05 M *n*-Bu_4NPF_6 as a supporting electrolyte, Pt electrode as working electrode, Pt

‡ In the case of $Sc_3N@I_h$-C_{80} derivative **4**, a 10^{-5} M solution has been used due to the reduced solubility of this fullerene derivative in *o*-DCB.

wire as counter electrode, $Ag/AgNO_3$ non-aqueous electrode as pseudo-reference electrode. Potential values are referred to $E_{(ox)1/2}$ of the Fc/Fc^+ redox couple (+0.30 V in the present conditions).

4. Job plots experiments on 2/3 complex

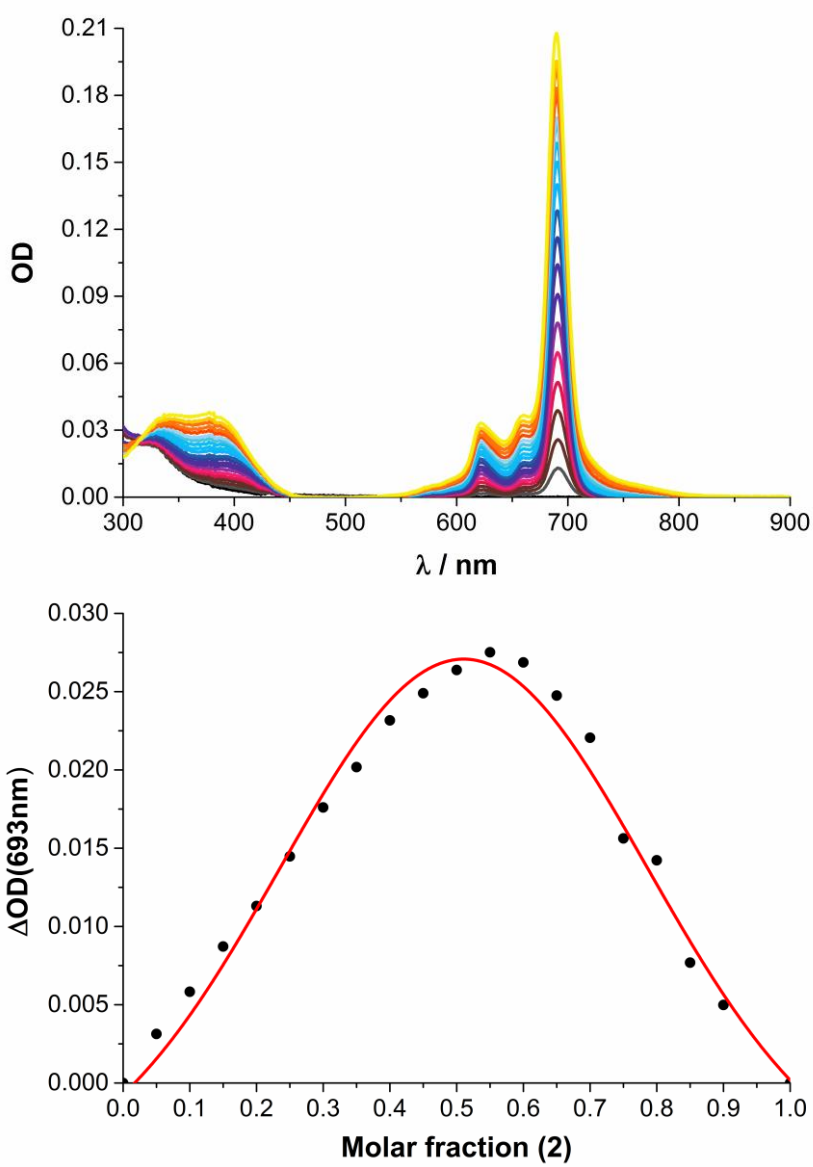

Figure S18. Top: UV-vis absorption spectra obtained at different **2**/**3** ratios (from 0 (black spectrum) to 1 (yellow spectrum) at 0.05 increment) in chlorobenzene (total concentration = 1.0 x 10^{-6} M). Bottom: Job plot analysis for the complexation of electron-deficient Zn(II)Pc **2** with C_{60} derivative **3** in chlorobenzene monitored at 693 nm.

5. Fluorescence titration measurements on 1/3 and 2/3 complexes

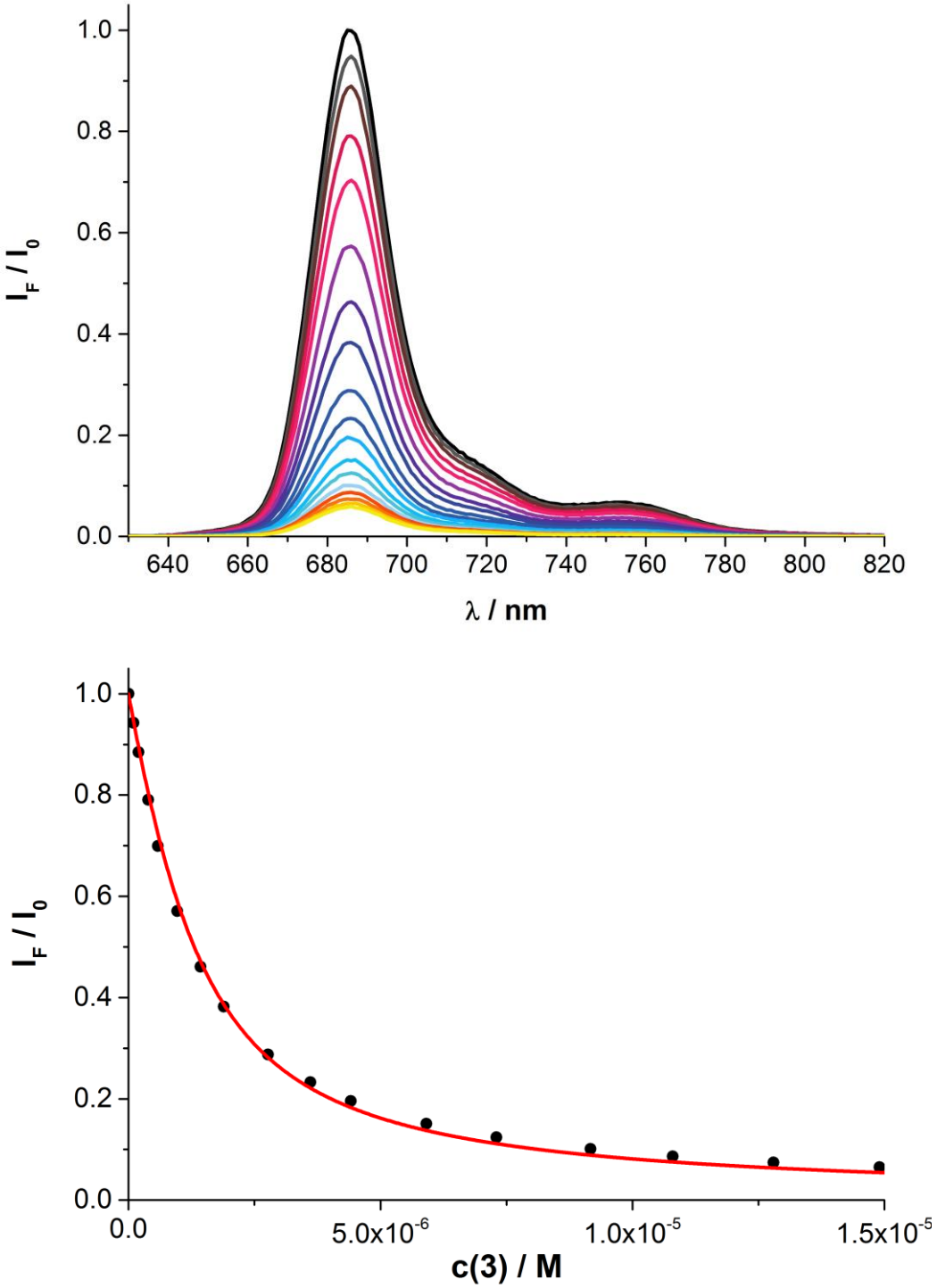

Figure S19. (Top) Steady-state fluorescence spectra (λ_{exc} = 610 nm) of electron-rich Zn(II)Pc **1** (c = 1.0 x 10^{-6} M) upon addition of C_{60} derivative **3** (from 0 (black spectrum) up to 1.7 x 10^{-5} M (yellow spectrum)) in argon-saturated chlorobenzene at room temperature. (Bottom) Plot of the change in fluorescence intensity at 685 nm as a ratio of I_F/I_0 *versus* the concentration of C_{60} derivative **3**. The solid line shows the estimated curve-fit (with an R value of 0.99862) obtained by non-linear least-squares analysis.

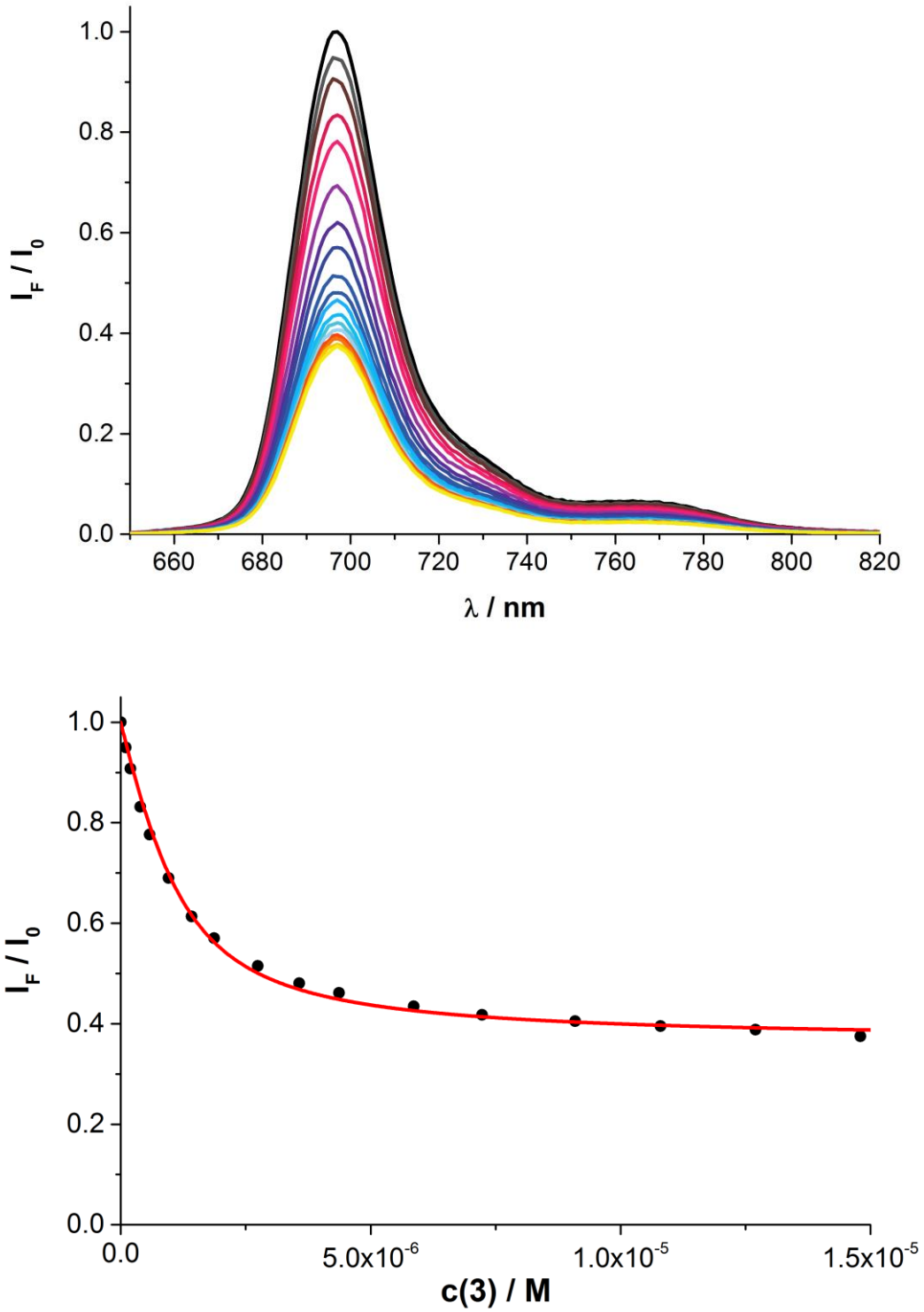

Figure S20. (Top) Steady-state fluorescence spectra (λ_{exc} = 630 nm) of electron-deficient Zn(II)Pc **2** (c = 1.0 x 10^{-6} M) upon addition of C_{60} derivative **3** (from 0 (black spectrum) up to 1.7 x 10^{-5} M (yellow spectrum)) in argon-saturated chlorobenzene at room temperature. (Bottom) Plot of the change in fluorescence intensity at 695 nm as a ratio of I_F/I_0 *versus* the concentration of C_{60} derivative **3**. The solid line shows the estimated curve-fit (with an R value of 0.99685) obtained by non-linear least-squares analysis.

6. Spectroelectrochemical studies on derivatives 1 and 4

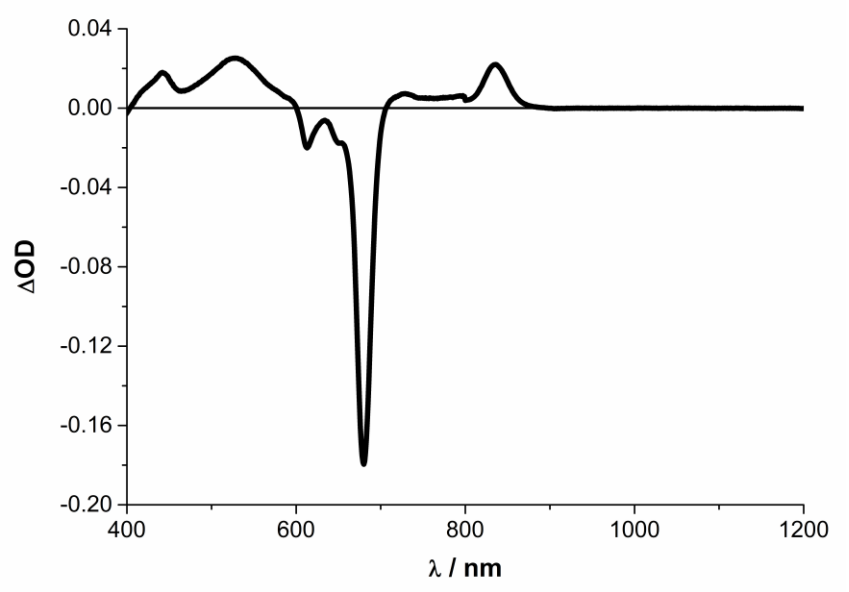

Figure S21. Differential absorption spectra (visible and near-infrared) obtained upon electrochemical oxidation of electron-rich Zn(II)Pc **1** (applied bias of +0.5 V) in argon-saturated *o*-DCB at room temperature with 0.05 M *n*-Bu_4NPF_6 as supporting electrolyte and silver-wire as pseudo-reference electrode.

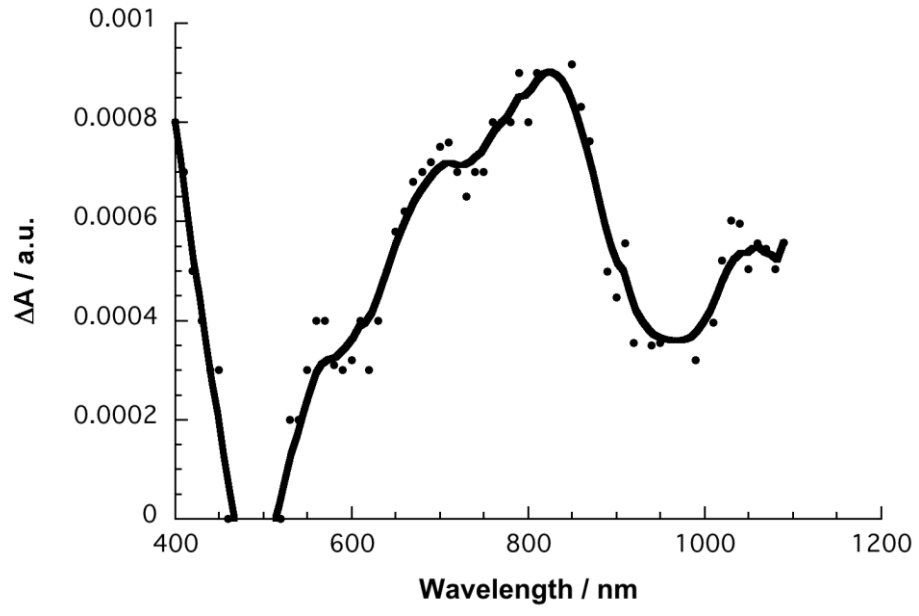

Figure S22. Differential absorption spectrum following pulse radiolytic reduction of $Sc_3N@I_h$-C_{80} derivative **4** in a deoxygenated solvents mixture containing toluene, 2-propanol and acetone with $(CH_3)_2$•COH and $(CH_3)_2$•CO^- radicals.[3]

7. Femtosecond laser flash photolysis studies on derivatives 1, 2, 3 and 4, and supramolecular complexes 1/3 and 2/3

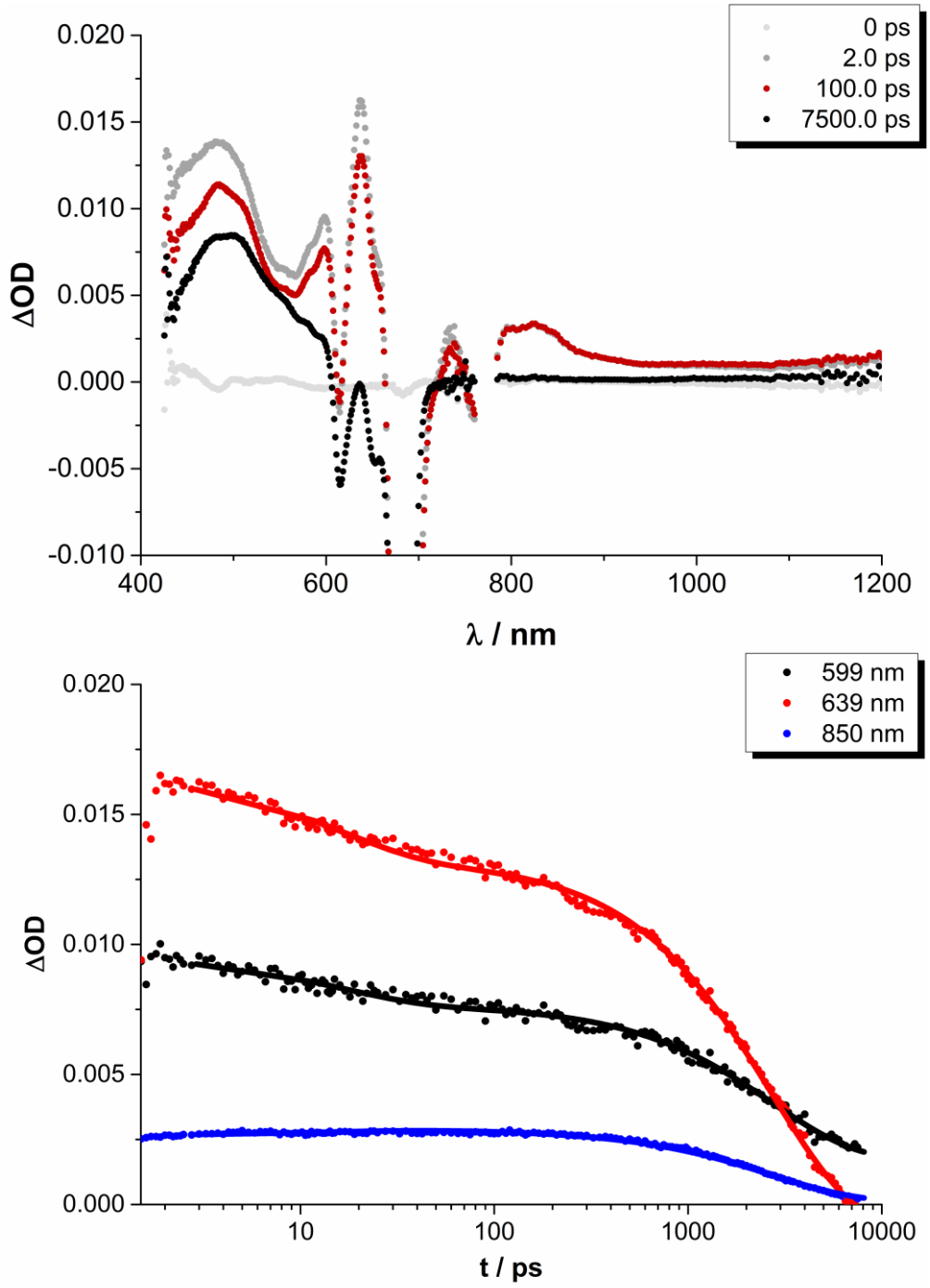

Figure S23. (Top) Differential absorption spectra (visible and near-infrared) obtained upon femtosecond flash photolysis (676 nm) of electron-rich Zn(II)Pc **1** (c = 1 x 10^{-5} M) in argon-saturated chlorobenzene with several time delays of 0 ps (ground state), 2 (singlet excited state), 100 ps (transition between singlet and triplet excited state), and 7500 ps (triplet excited state) at room temperature. (Bottom) Time-absorption profiles of the spectra shown above at 599 nm (black), 639 nm (red), and 850 nm (blue) monitoring intrinsic Zn(II)Pc intersystem crossing (2.8 ± 0.1 ns).

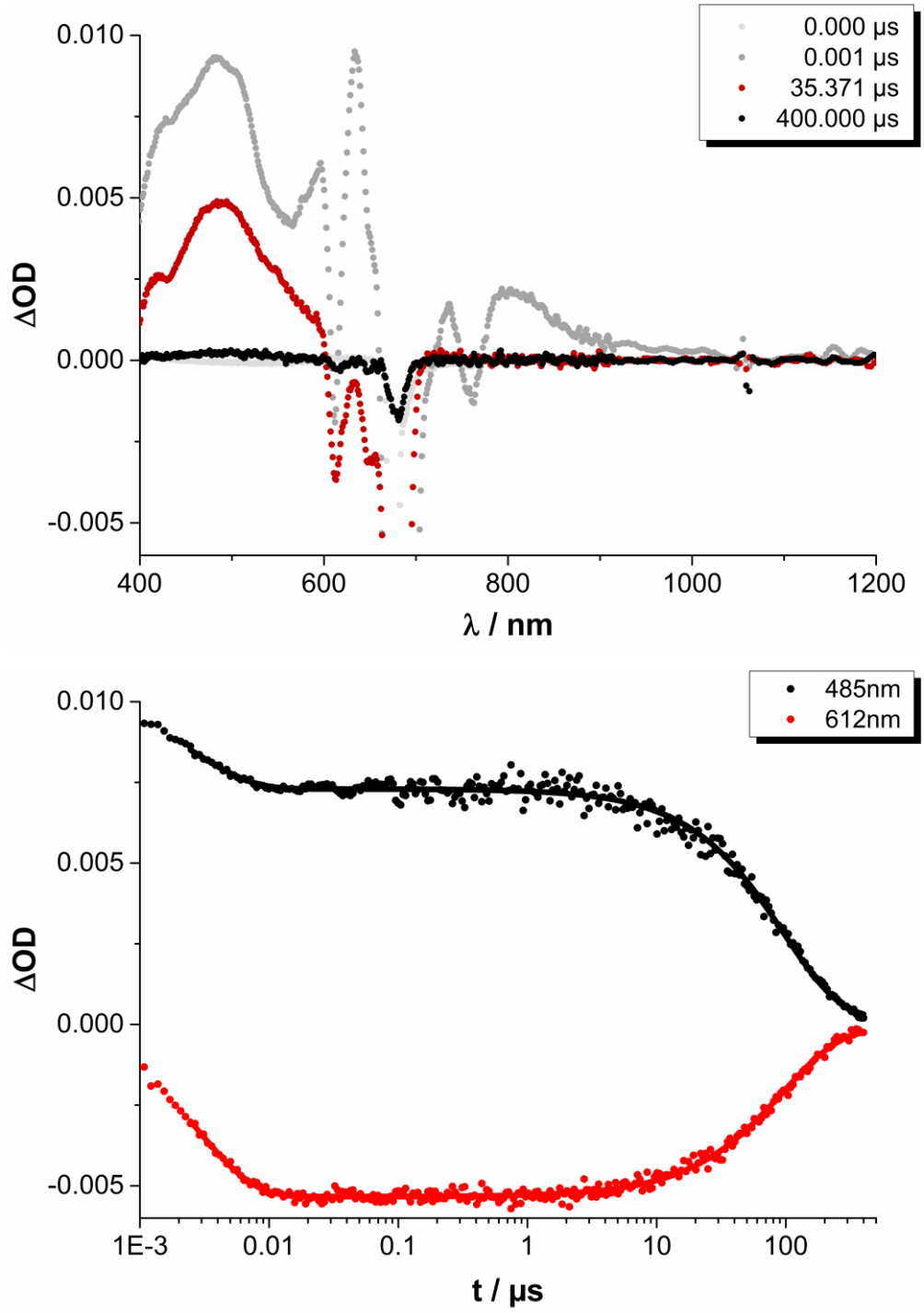

Figure S24. (Top) Differential absorption spectra (visible and near-infrared) obtained upon nanosecond flash photolysis (676 nm) of electron-rich Zn(II)Pc **1** (c = 1 x 10^{-5} M) in argon-saturated chlorobenzene with several time delays of 0 µs (ground state), 0.001 (singlet excited state) as well as 35 and 400 µs (triplet excited state) at room temperature. (Bottom) Time-absorption profiles of the spectra shown above at 485 nm (black) and 612 nm (red) monitoring intrinsic Zn(II)Pc intersystem crossing (97 ± 2 µs).

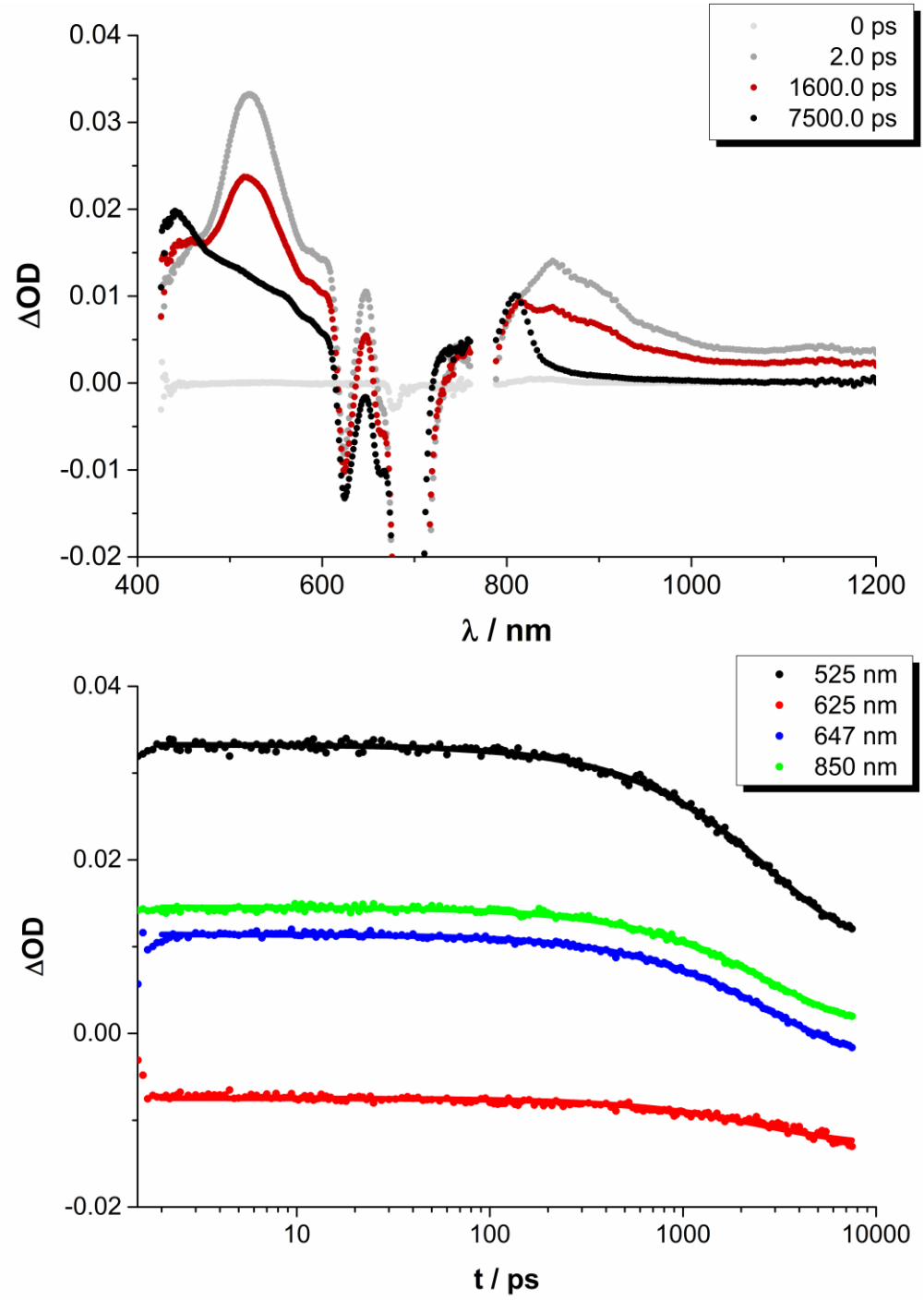

Figure S25. (Top) Differential absorption spectra (visible and near-infrared) obtained upon femtosecond flash photolysis (676 nm) of electron-deficient Zn(II)Pc **2** (c = 1 x 10^{-5} M) with a drop of pyridine to circumvent Zn(II)Pcs' aggregation in argon-saturated chlorobenzene with several time delays of 0 ps (ground state), 2 ps (singlet excited state), 1600 ps (transition between singlet and triplet excited state), and 7500 ps (triplet excited state) at room temperature. (Bottom) Time-absorption profiles of the spectra shown above at 525 nm (black), 625 nm (red), 647 nm (blue), and 850 nm (green) monitoring intrinsic Zn(II)Pc intersystem crossing (2.8 ± 0.1 ns).

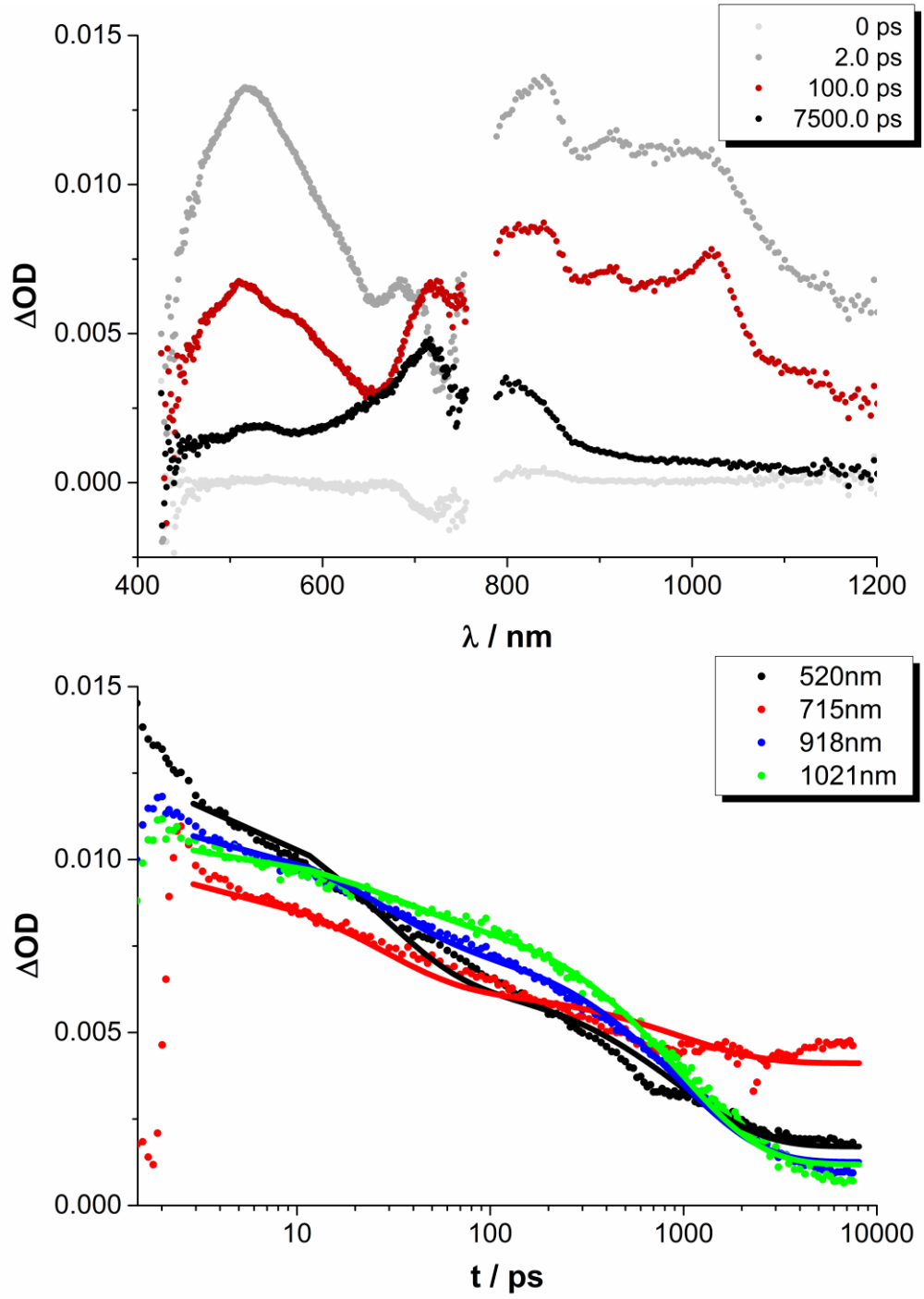

Figure S26. (Top) Differential absorption spectra (visible and near-infrared) obtained upon femtosecond flash photolysis (387 nm) of C_{60} derivative **3** (c = 1 x 10^{-5} M) in argon-saturated chlorobenzene with several time delays of 0 ps (ground state), 2 ps (singlet excited state), 100 ps (transition between singlet and triplet excited state), and 7500 ps (triplet excited state) at room temperature. (Bottom) Time-absorption profiles of the spectra shown above at 520 nm (black), 715 nm (red), 918 nm (blue), and 1021 nm (green) monitoring intrinsic C_{60} intersystem crossing (1.5 ± 0.1 ns).

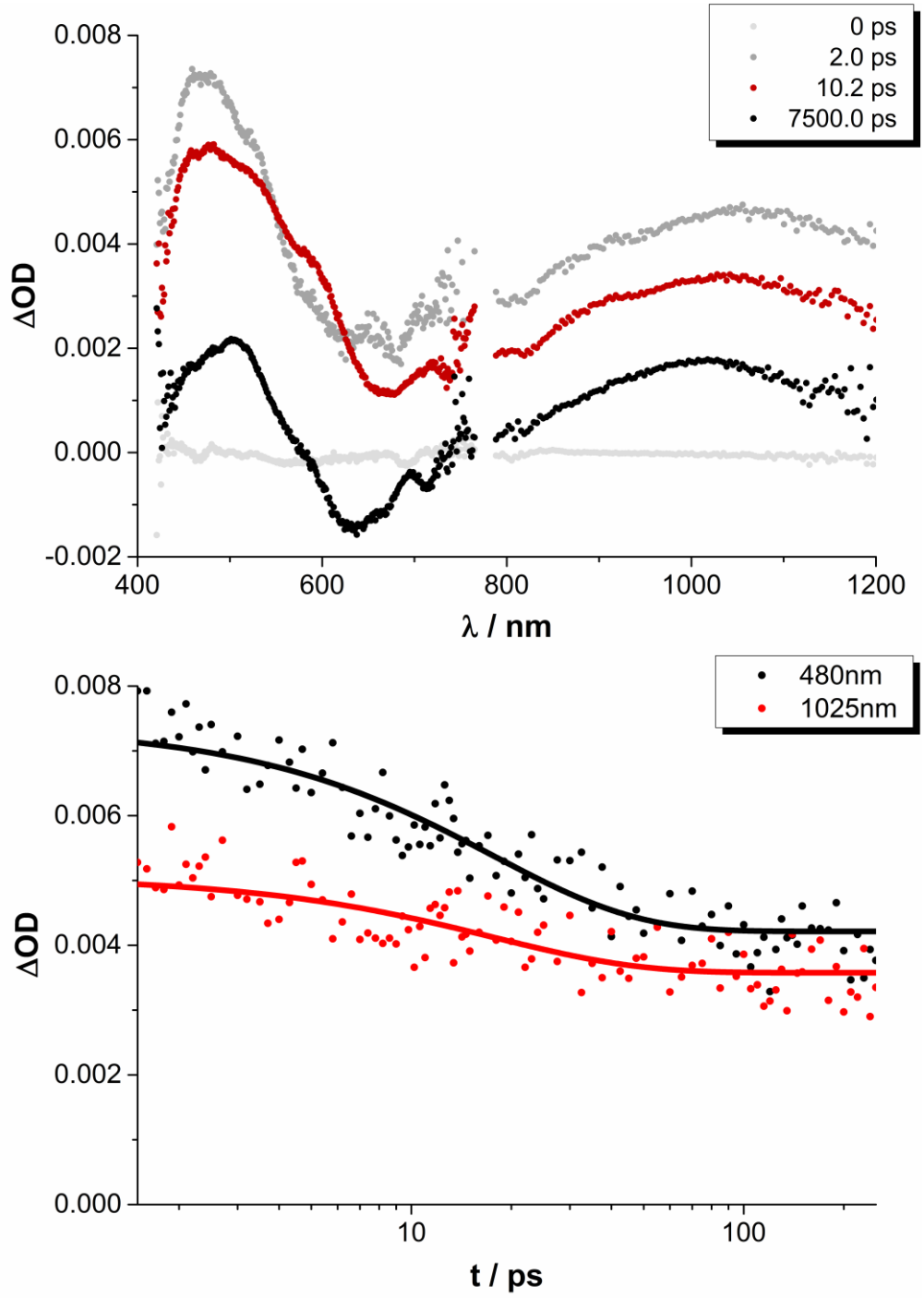

Figure S27. (Top) Differential absorption spectra (visible and near-infrared) obtained upon femtosecond flash photolysis (387 nm) of $Sc_3N@I_h$-C_{80} derivative **4** (c = 1 x 10^{-5} M) in argon-saturated chlorobenzene with several time delays of 0 ps (ground state), 2 ps (singlet excited state), 10.2 ps (transition between singlet and triplet excited state), and 7500 ps (triplet excited state) at room temperature. (Bottom) Time-absorption profiles of the spectra shown above at 480 nm (black) and 1025 nm (red) monitoring intrinsic $Sc_3N@I_h$-C_{80} intersystem crossing (25 ± 5 ps).

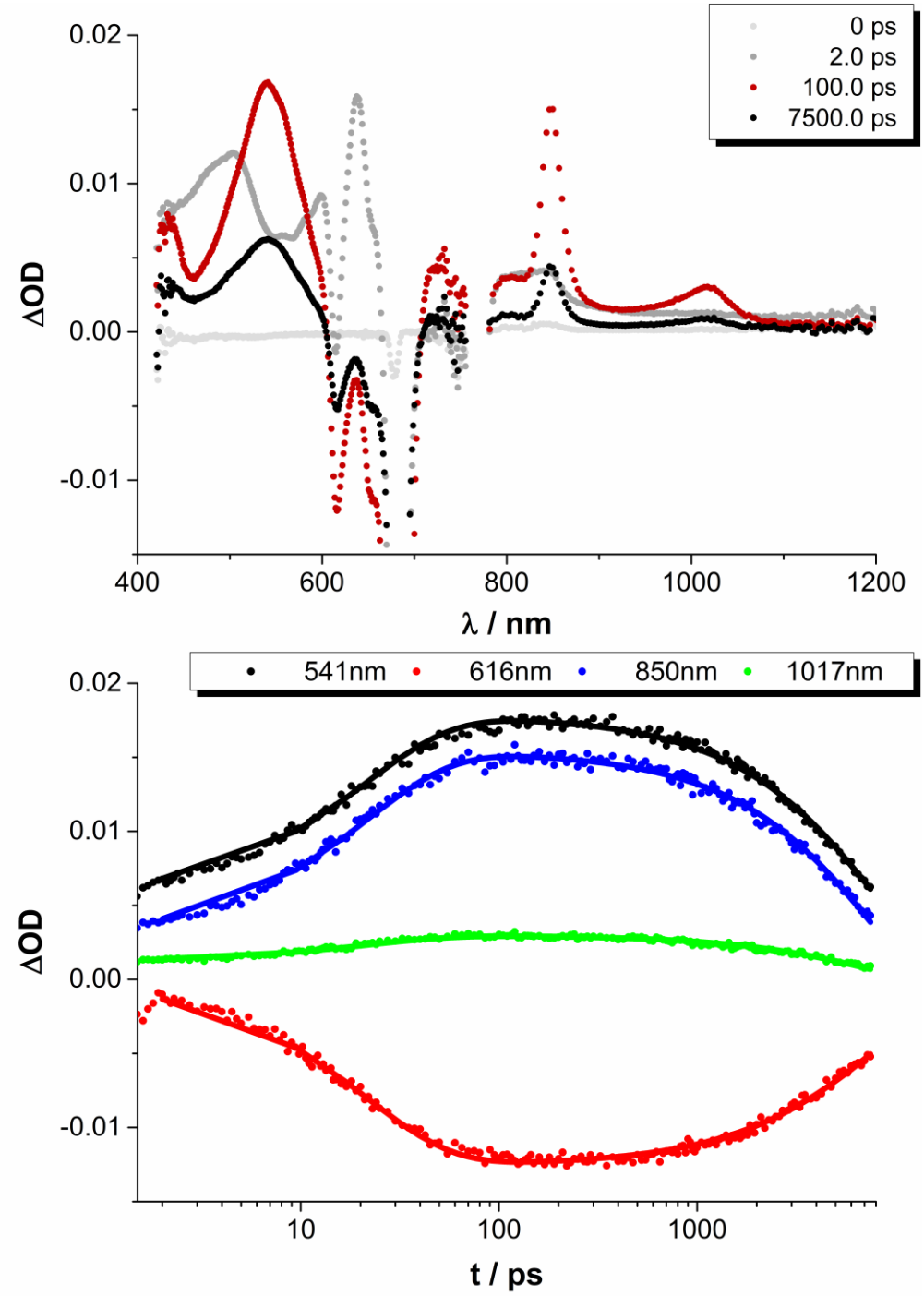

Figure S28. (Top) Differential absorption spectra (visible and near-infrared) obtained upon femtosecond flash photolysis (676 nm) of **1**/**3** (ratio between **3** and **1** = 10) in argon-saturated chlorobenzene with several time delays of 0 ps (ground state), 2 ps (singlet excited state), 100, and 7500 ps (radical ion pair state) at room temperature. (Bottom) Time-absorption profiles of the spectra shown above at 541 nm (black), 616 nm (red), 850 nm (blue), and 1017 nm (green) monitoring the charge separation (29 ± 1 ps) and the charge recombination kinetics (9.0 ± 0.5 ns).

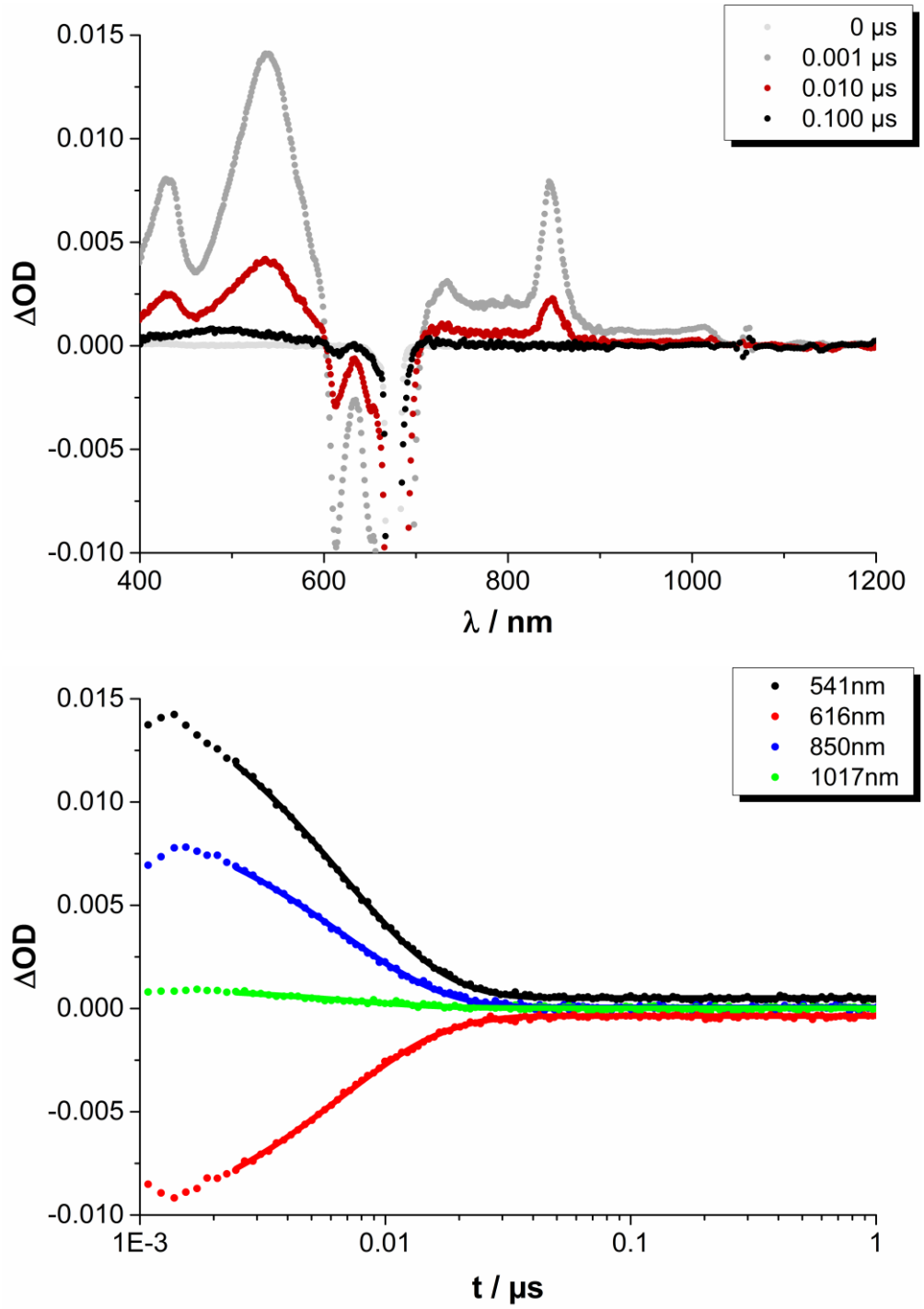

Figure S29. (Top) Differential absorption spectra (visible and near-infrared) obtained upon nanosecond flash photolysis (676 nm) of **1**/**3** (ratio between **3** and **1** = 10) in argon-saturated chlorobenzene with several time delays of 0 µs (ground state), 0.001, 0,01 µs (radical ion pair state), and 0.1 µs (ground state, the Zn(II)Pc triplet excited state features observed at 0.1 µs likely result from uncomplexed Zn(II)Pc **1** in solution) at room temperature. (Bottom) Time-absorption profiles of the spectra shown above at 541 nm (black), 616 nm (red), 850 nm (blue), and 1017 nm (green) monitoring the charge recombination kinetics (6.6 ± 0.5 ns).

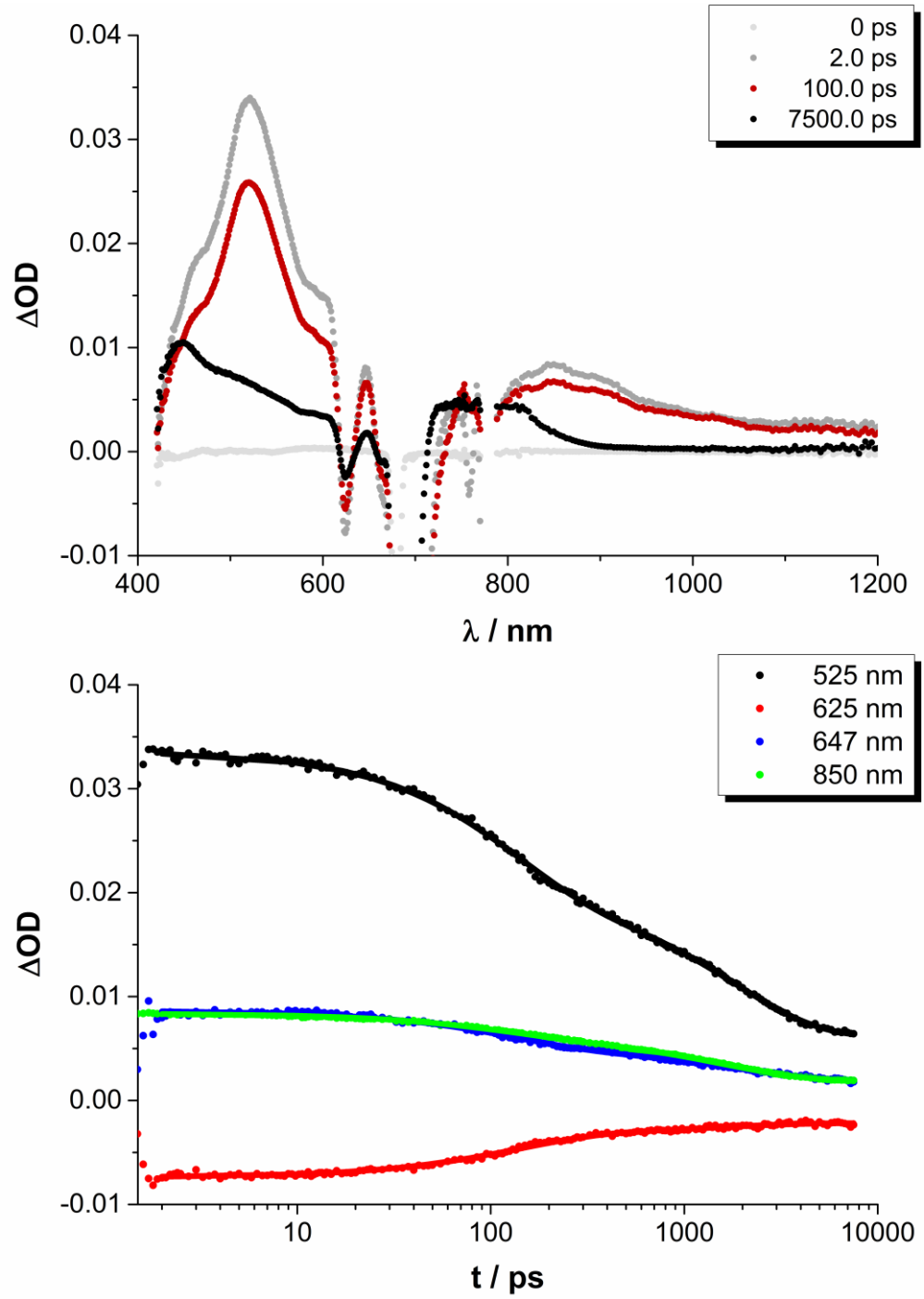

Figure S30. (Top) Differential absorption spectra (visible and near-infrared) obtained upon femtosecond flash photolysis (676 nm) of supramolecular ensemble **2**/**3** (ratio between **3** and **2** = 10) in argon-saturated chlorobenzene with several time delays of 0 ps (ground state), 2 ps (singlet excited state), 100 ps (transition between singlet and triplet excited state), and 7500 ps (triplet excited state) at room temperature. (Bottom) Time-absorption profiles of the spectra shown above at 525 nm (black), 625 nm (red), 647 nm (blue), and 850 nm (green) monitoring intrinsic Zn(II)Pc intersystem crossing (2.8 ± 0.1 ns).

8. References section

1 Tat, F. T.; Zhou, Zh.; MacMahon, Sh.; Song, F.; Rheingold, A. L.; Echegoyen, L.; Schuster, D. I.; Wilson, S. R. *J. Org. Chem.* **2004**, *69*, 4602–4606.

2 Ceron, M. R.; Li, F.-F.; Echegoyen, L. *Chem. Eur. J.* **2013**, *19*, 7410–7415.

3 Pinzón, J. R.; Cardona, C. M.; Herranz, M. Á.; Plonska-Brzezinska, M. E.; Palkar, A.; Athans, A. J.; Martín, N.; Rodríguez-Fortea, A.; Poblet, J. M.; Bottari, G.; Torres, T.; Gayathri, S. S.; Guldi, D. M.; Echegoyen, L. *Chem. Eur. J.* **2009**, *15*, 864–877.